(2)

NAVAL POSTGRADUATE SCHOOL
Monterey, California

THESIS

THE ROLES OF STRAIN AND REHEATING INTERVAL IN CONTINUOUS RECRYSTALLIZATION DURING THE THERMOMECHANICAL PROCESSING BY WARM ROLLING OF AN AL-MG ALLOY

by

Thomas E. Gorsuch

December 1989

Thesis Advisor T. R. McNelley

Unclassified

Security Classification of this page

REPORT DOCUMENTATION PAGE

1a Report Security Classification Unclassified	1b Restrictive Markings
2a Security Classification Authority	3 Distribution Availability of Report
2b Declassification/Downgrading Schedule	Approved for public release; distribution is unlimited.
4 Performing Organization Report Number(s)	5 Monitoring Organization Report Number(s)
6a Name of Performing Organization: Naval Postgraduate School	6b Office Symbol (*If Applicable*) 34
6c Address (*city, state, and ZIP code*): Monterey, CA 93943-5000	7a Name of Monitoring Organization: Naval Postgraduate School
	7b Address (*city, state, and ZIP code*): Monterey, CA 93943-5000
8a Name of Funding/Sponsoring Organization	8b Office Symbol (*If Applicable*)
8c Address (*city, state, and ZIP code*)	9 Procurement Instrument Identification Number
	10 Source of Funding Numbers

Program Element Number	Project No	Task No	Work Unit Accession No

11 Title (*Include Security Classification*) THE ROLES OF STRAIN AND REHEATING INTERVAL IN CONTINUOUS RECRYSTALLIZATION DURING THE THERMOMECHANICAL PROCESSING BY WARM ROLLING OF AN AL-10MG ALLOY

12 Personal Author(s) Thomas E. Gorsuch

13a Type of Report	13b Time Covered		14 Date of Report (*year, month,day*)	15 Page Count
	From	To		
Master's Thesis			December 1989	79

16 Supplementary Notation The views expressed in this thesis are those of the author and do not reflect the official policy or position of the Department of Defense or the U.S. Government.

17 Cosati Codes			18 Subject Terms (*continue on reverse if necessary and identify by block number*)
Field	Group	Subgroup	superplasticity, Aluminum-Magnesium alloys, continuous recrystallization, Theses, Deformation, Aerospace Industry, TMP (JG)

19 Abstract (*continue on reverse if necessary and identify by block number*)

Investigation into the influence of rolling strain and into the variation of properties and structure during reheating intervals between rolling passes in the thermomechanical processing of an Al-9.89Mg-0.09Zr alloy (composition in weight percent) was conducted. Superplastic ductilities up to approximately 1120 percent were achieved by processing to a total strain of 2.5 utilizing a reheating interval of 30 minutes. Conversely, rolling to lesser values of strain with the same reheating interval or rolling to a strain of 2.5 and using a 5 minute reheating interval produced ductilities less than 400 percent. A strong correlation was demonstrated between results achieved and a qualitative model for continuous recrystallization during thermomechanical processing previously proposed.

20 Distribution/Availability of Abstract	21 Abstract Security Classification
[X] unclassified/unlimited [ ] same as report [ ] DTIC users	Unclassified

22a Name of Responsible Individual	22b Telephone (*Include Area code*)	22c Office Symbol
T.R. McNelley	(408) 646-2589	69Mc

DD FORM 1473, 84 MAR 83 APR edition may be used until exhausted

All other editions are obsolete

security classification of this page Unclassified

Approved for public release; distribution is unlimited.

The Roles of Strain and Reheating Interval in Continuous Recrystallization During the Thermomechanical Processing by Warm Rolling of an Al-Mg Alloy

by

Thomas E. Gorsuch
Lieutenant Commander, United States Navy
B.S.N.E., University of Virginia, 1976

Submitted in partial fulfillment of the requirements
for the degree of

MASTER OF SCIENCE IN ENGINEERING SCIENCE

from the

NAVAL POSTGRADUATE SCHOOL
December 1989

Author: _____
Thomas E. Gorsuch

Approved by: _____
T.R. McNelley, Thesis Advisor

_____
Anthony J. Healey, Chairman, Department of Mechanical Engineering

ABSTRACT

Investigation into the influence of rolling strain and into the variation of properties and structure during reheating intervals between rolling passes in the thermomechanical processing of an Al-9.89Mg-0.09Zr alloy (composition in weight percent) was conducted. Superplastic ductilities up to approximately 1120 percent were achieved by processing to a total strain of 2.5 utilizing a reheating interval of 30 minutes. Conversely, rolling to lesser values of strain with the same reheating interval or rolling to a strain of 2.5 and using a 5 minute reheating interval produced ductilities less than 400 percent. A strong correlation was demonstrated between results achieved and a qualitative model for continuous recrystallization during thermomechanical processing previously proposed.

TABLE OF CONTENTS

LIST OF FIGURES

ACKNOWLEDGMENTS

I would like to express my sincere gratitude to Professor Terry McNelley for providing his insightful guidance and direction in this research endeavor. I wish to thank Mr. Tom Kellogg, Mr. Rob Hafley, Mr. Tom McCord, and Dr. Peter Kalu for their technical support. A special thank-you to my wife Paula, and my children, Tory and Matt, for their patience, understanding and encouragement during my studies at the Naval Postgraduate School.

I. INTRODUCTION

The ability of some metallic materials to deform to extremely large neck-free elongation under particular conditions of temperature and strain rate is termed superplasticity. Most alloys of given composition are not naturally superplastic. The microstructure of the alloy must be refined through thermomechanical processing (TMP) to develop the requisite characteristics to deform superplastically. Small modifications in the thermomechanical processing and/or alloy composition may result in drastic changes in the superplastic characteristics of the resulting material.

The aerospace industry has always been on the forefront of technology, especially when the object is to get more payload into the air. Improvements in strength, ductility, and toughness, along with resistance to fatigue and corrosion, and reduced weight of components have been general goals in the search for new materials. Because of their potentially high strength-to-weight ratio combined with low density, Aluminum alloys are the predominant materials of airframe construction involving beam structures and sheet metal components.

Superplastic forming has been commercially applied to Aluminum and Titanium alloys. The ability to form complex shapes with great precision in a few operations using relatively inexpensive tooling equates to reduced costs and improved performance in comparison to conventional forming techniques for complex structures. In particular, superplastic forming offers the ability to form in one piece a shape which would involve the joining of a large number of individual pieces with conventional methods. The complex, superplastically

formed shapes have meant fewer fasteners which reduces weight, eliminates a source of stress concentrators and increases corrosion resistance. Especially in the marine environment, superplasticity offers benefits which serve to spur research sponsored by the Department of the Navy.

Though the phenomenon of superplasticity was reported as long ago as 1912 by Bengough (Reference 1: pp. 123-147), real interest was not stimulated until a review of work in the USSR since World War II was published by Underwood (Reference 2: pp. 914-919) in 1962. Initially thought to be confined to eutectic alloys because of the ability to produce a fine grained matrix in which growth is limited by second phase particles, superplasticity has been found in other, more dilute alloys (Reference 3: pp. 189-190) . It is acknowledged that the prerequisite for superplastic deformation is an equiaxed, fine grain structure which remains stable at the deformation temperature. Control of the microstructure is essential to the application of superplasticity.

Along with the Naval Air Development Center, the Naval Postgraduate School is investigating superplasticity in Aluminum alloys including, high Magnesium content Aluminum-Magnesium and Aluminum-Magnesium-Lithium alloys. The focus of this thesis is to gain further insight into the effect of annealing interval and the strain to which the material is deformed during the TMP of a high Magnesium content Aluminum Alloy.

II. BACKGROUND

Aluminum ranks second only to iron and steel in terms of volume and weight used industrially, (Reference 4: p.6.1) with Aluminum-Magnesium (Al-Mg) alloys making up nearly half the total production by tonnage. Alloys can be classified into two groups: non-heat-treatable and heat-treatable, based upon the method of strengthening employed. Precipitation hardening is the strengthening mechanism for heat-treatable Al alloys, while solution hardening, in combination with strain hardening, is the mechanism for non-heat-treatable alloys.

A. STRENGTHENING MECHANISMS

In pure metals, dislocations can move readily through the material imparting little strength and easily allowing plastic deformation. By restraining the dislocation movement the material is strengthened.

1. Solid Solution Strengthening

Introducing solute atoms into the crystal lattice, the solute atoms interact with dislocations restricting their motion and strengthening the material. All Al alloys are strengthened to some degree by the solid solution mechanism. The addition of Mg to Al contributes substantial solid solution strengthening due to the size difference between Al and Mg atoms and the resultant interaction between the Mg and dislocations in the alloy.

2. Precipitation

In many Al alloys the precipitation of a second phase may provide some strengthening. However, in Al-Mg alloys the precipitate described as (Reference 5: p.312) :

$$\text{Supersaturated Solution} \rightarrow \text{Al} + \beta\ (Mg_5Al_8)$$

does not provide a coherent precipitate in the matrix, but rather an incoherent phase which forms with preference for grain boundaries. Though the ß phase precipitate does not provide for direct strengthening, it is instrumental in achieving the superplastic response when distributed uniformly as fine particles which stabilize an evolving substructure.

3. Dispersion Strengthening

Particles which are much harder than the surrounding matrix and are insoluble at even high temperatures are termed dispersoids and the material is dispersion hardened . The particles are of fine size and are incoherent in the matrix. Ambient strength is added to the material by inhibiting recrystallization. The addition of Zirconium (Zr) to the Al alloy causes a second phase particle $ZrAl_3$ to be precipitated at high temperature. As a dispersoid, $ZrAl_3$ increases the recrystallization temperature (Reference 5: p.414) and aids in controlling recrystallization during processing (Reference 6: p.2320) to achieve the fine grain structure necessary for superplasticity.

B. DEVELOPMENT OF SUPERPLASTICITY

1. Grain Refinement

It is generally recognized that grain refinement is necessary for superplasticity. An optimum size of 1 to 2 μm is desired to facilitate forming at reduced temperatures and also to diminish cavitation during forming. Grain refinement is more easily accomplished in a two phase structure. The Al alloy utilized in this study at the NPS has a sufficiently high content of Mg to produce the second phase through the sequence of solution treatment above the solvus followed subsequently by warm working below the solvus temperature (Figure 1) . The precipitate, when present in sufficient quantities and of sufficient size, enhances grain refinement when uniformly distributed throughout the matrix (Reference 7: p.367) . With a sequential series of warm rolling passes and static annealing intervals, dislocation generation and dynamic recovery alternate with the second phase precipitation (Reference 8) . A process of continuous recrystallization occurs by the precipitation of a fine, intermetallic second phase precipitate produced concurrently with a highly refined subgrain structure. The precipitate acts as a stabilizing agent by pinning the subgrain structure and prevents recrystallization by boundary migration and thus maintains the structure in a metastable state (Reference 9) .

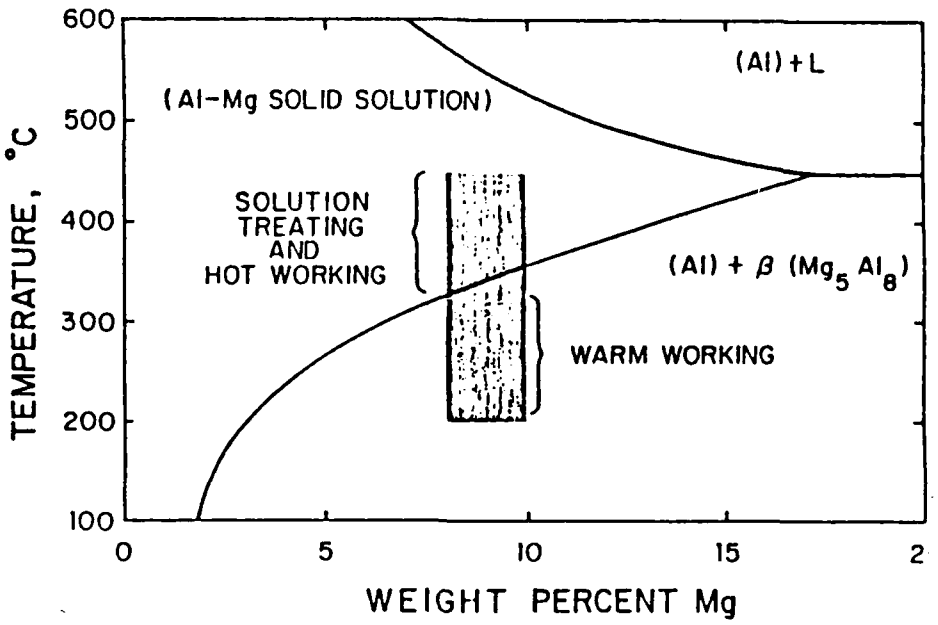

Figure 1. Al-Mg-Zr Phase Diagram Showing TMP Region

In the initial stages of annealing, continuous recrystallization transforms a dislocation cell structure into subgrains. The migration rate of dislocations determines the reaction rate. Later, the reaction rate depends on the rate of coalescence of the subgrains (Reference 10) . Thus, a high initial dislocation density will result in a larger misorientation of the subgrain boundaries which, in turn, causes a higher rate of reaction by deminishing the repulsion of a boundary for nearby matrix dislocations.

During the process of cyclic warm rolling and annealing, recovery will increase the low angles of misorientation of the subgrains into progressively higher misorientations (on the order of five to seven degrees) which permit the necessary grain boundary sliding of superplastic deformation to occur (Reference 11: p.1237) . The use of relatively long (approximately 30 minutes

or longer) reheating intervals allows the high dislocation density of the initial rolling pass to form a subgrain structure. The second (and subsequent) rolling passes re-introduce a high dislocation density which then recovers to the pre-existing subgrain structure. The migration of the dislocations into the subgrain boundaries reduces the spacing between the dislocations in the boundaries (Figure 2) . The magnitude of the stress fields associated with the boundaries decreases as the dislocation spacing decreases and the misorientation of the boundaries increases (Reference 10) . As the misorientations are increased by the continued absorbtion of dislocations in each rolling and annealing cycle, the resulting boundaries eventually obtain a character necessary to support superplastic deformation. The use of short annealing intervals between rolling passes does not allow sufficient time for the subgrain structure to adequately develop. The resulting microstructure is of finer grain size and of low misorientation angle . At the end of each cycle there remains a relatively high dislocation density within the grains (Figure 3) . (Reference 10)

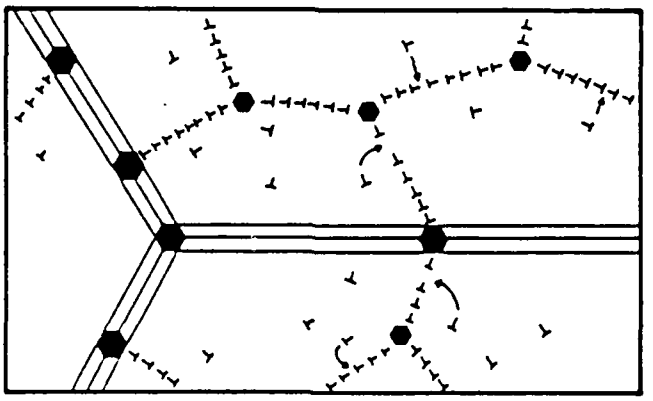

(a)

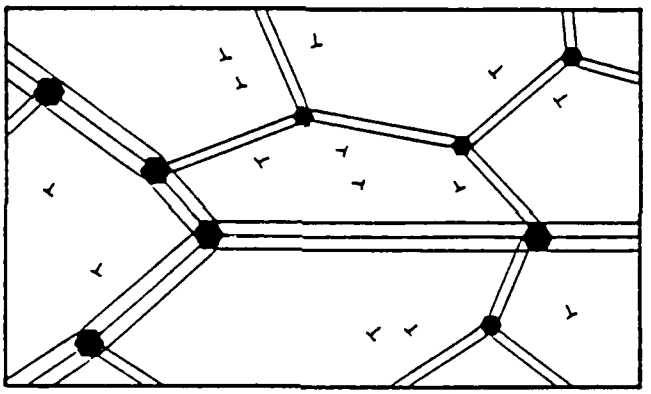

(b)

Figure 2. Moderate Angle Boundary Buildup With Long Annealing Intervals : (a) in early rolling passes, precipitation of the ß phase pins dislocations, forming subgrain boundaries. (b) In subsequent cycles the long annealing interval allows further dislocation migration until the resultant structure consists of moderate angle boundaries in which individual dislocations are no longer discernable (from model by Hales, McNelley, & McQueen reprinted by permission) .

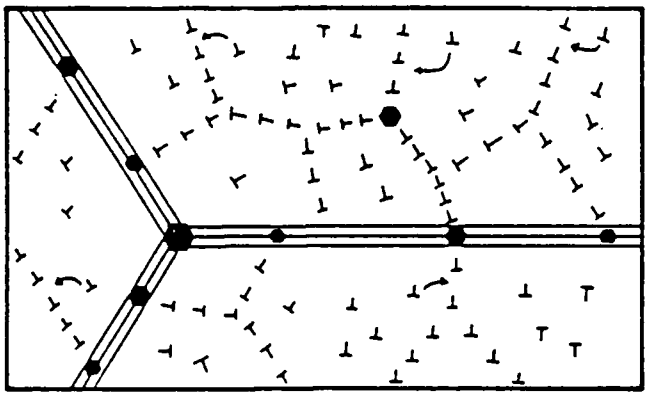

(a)

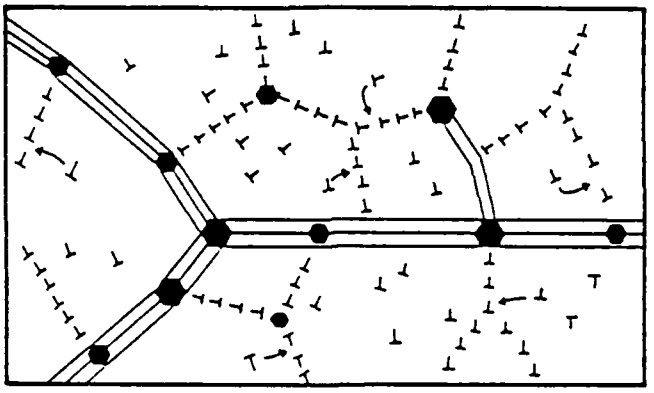

(b)

Figure 3. Short Annealing Interval Effect on Substructure Buildup : (a) during early rolling - annealing cycles there is less precipitation of ß phase and structure consists of finer grains. (b) The short annealing interval does not allow sufficient time for dislocations induced in subsequent cycles to migrate completely to the boundary (from model by Hales, McNelley, & McQueen reprinted by permission) .

2. Mechanisms of Superplastic Flow

All superplastic materials have shown a common characteristic: the relation of flow stress to strain rate according to the relation :

$$\sigma = \kappa \dot{\varepsilon}^m \tag{1}$$

where s is the flow stress, $\dot{\varepsilon}$ is the strain rate and κ and m are material constants. As the value of m increases towards unity, the greater becomes the ability for superplastic response. The coefficient m is referred to as the strain rate sensitivity coefficient (Reference 11: p.1229) and materials exhibiting values of $m \approx 0.5$ have displayed ductilities over 1000% . The higher the value of m the greater the suppression of localized necking. The onset of necking can be shown to correspond to the condition :

$$m + \gamma \leq 1 \tag{2}$$

where γ is the dimensionless strain hardening coefficient given by :

$$\gamma = (1 / \sigma) / (\partial \sigma / \partial \varepsilon) . \tag{3}$$

The value of m can be determined from double logrithmic plots of flow stress vs. strain rate by :

$$m = \partial \ln \sigma / \partial \ln \dot{\varepsilon} \tag{4}$$

and predictions of the strain rate to support maximum ductility can be made (Reference 12 : pp. 297, 308) . The coefficient γ will ultimately tend to zero and the implication for superplastic deformation where m is approximately 0.5 is that the onset of necking is inhibited and localized necking does not occur.

A value of m approaching 0.5 or greater is not the sole requirement for superplasticity. Embrittlement of grain boundaries and cavitation at boundaries can cause failure even when the value of m is high (Reference 13 : p.832) . Also, microstructural coarsening during superplastic deformation may result in changes in deformation mechanisms and corresponding changes in the value of the coefficients m and γ .

III. EXPERIMENTAL PROCEDURE

A. CASTING AND SECTIONING

Casting number S572826, provided by the ALCOA Technical Center, ALCOA Center, Pennsylvania, and of composition Al - 9.89Mg - 0.09Zr was received in cast form with dimensions 6in. diameter x 23in. length (150mm dia. x 580mm length.). A part of the casting was sectioned into nine billets for subsequent solution treatment and processing. The billet dimensions were 3.75 in. x 1.25 in. x 1.25 in. (95.3 mm x 31.8 mm x 31.8 mm).

B. THERMOMECHANICAL PROCESSING

Solution treatment for 24 hours at 440°C was accomplished for homogenization utilizing a Lindberg type B-6 Heavy Duty furnace. Upset forging the billet at 440°C was performed in a Baldwin - Tate - Emery testing machine equipped with heated platens. The billet was forged along the longitudinal axis to result in a 3.75:1 reduction to a final thickness of approximately one inch (2.54 cm.) . The forged billets were replaced in the 440°C furnace for one hour then quenched in water. The billets were sectioned to "square" the sides to reduce the possibility of edge cracking during rolling.

Thermomechanical processing (TMP) (Figure 4) was performed utilizing the parameters listed in Table 1. The rolling schedules were chosen to provide a means of studying the changes in dislocation density imparted to the billet as a function of annealing time between rolling passes and the number of passes (i.e. the total strain) taken.

The forged billet was placed in a Blue M Furnace, Model 8655-3 for the selected annealing interval prior to each rolling reduction. The length of the annealing interval was calculated as the time within the furnace and did not include the length of time (less than one minute) to transfer the billet to the rolling mill and return it to the furnace. A large steel plate was fitted to the bottom of the furnace to act as a heat capacitor in order to aid in maintaining a stable annealing temperature.

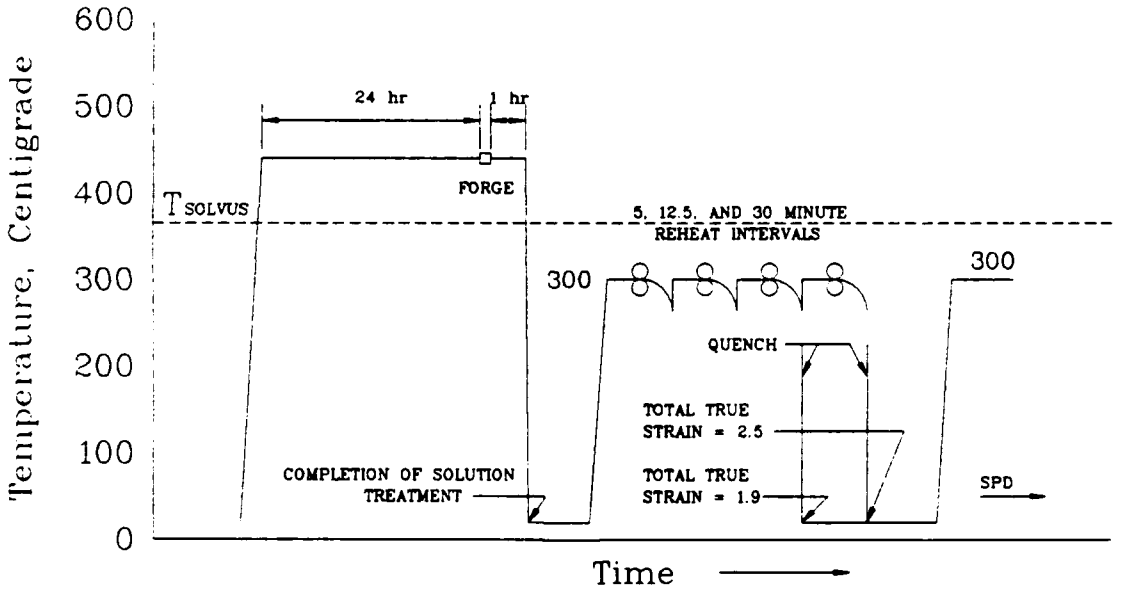

Figure 4. Thermomechanical Processing

TABLE 1. TMP PARAMETERS

TMP	Number of Rolling Passes	Annealing Interval
A	10 to $\varepsilon = 1.9$	5 min
B	10 to $\varepsilon = 1.9$	30 min
C	12 to $\varepsilon = 2.5$	5 min
D	12 to $\varepsilon = 2.5$	12.5 min
E	12 to $\varepsilon = 2.5$	30 min

The critical stage in producing a fine grained microstructure capable of superplastic deformation is the warm rolling. Five different TMP schemes were selected. The first two were designed to examine the affect of annealing interval on a billet reduced to $\varepsilon = 1.9$. The remaining three schedules varied the annealing interval on a billet reduced to a lesser strain ($\varepsilon=2.5$). Evaluation of the effect of strain can be made by comparison of materials processed by TMP's A and C or B and E.

Billets were rolled with a Fenn Laboratory Rolling Mill using the reduction schedules summarized in Table 2. As shown in the table, the strain per rolling pass generally increased with each successive rolling / annealing cycle. The rolling scheme commenced with a reduction of 10% in the first pass and the reduction per pass increased to about 30% in the latter rolling cycles. TMP's A and B utilized 10 passes to achieve a strain of 1.9 . TMP's C through E utilized all 12 passes to achieve 2.5 strain. The last rolling pass was followed by a water quench to room temperature.

TABLE 2. TMP ROLLING SCHEDULE

A. TMP'S A & B

Roll #	Roll Chg. (.08in+.01in)	Mill Set(L/R)	Mill Gap(in)	% Strain (per pass)
open	+(12 + 4)	0/0	.94	- -
1	- (2 + 0)	0/0	.84	10.4
2	- (1 + 2)	6/6	.74	12.0
3	- (1 + 2)	4/4	.64	13.5
4	- (1 + 2)	2/2	.54	15.6
5	- (1 + 2)	0/0	.44	18.5
6	- (1 + 2)	6/6	.34	22.7
7	- (1 + 2)	4/4	.24	29.4
8	- (0 + 6)	6/6	.18	25.0
9	- (0 + 5)	1/1	.13	27.7
10	- (0 + 4)	5/5	.09	30.7

B. ROLLING CONTINUED FOR TMP'S C-E

11	- (0 + 3)	2/2	.06	33.3
12	- (0 +1.3)	0.7/0.7	.047	21.7

C. TENSILE TESTING

A portion of the resulting strip was machined to dimensions for tensile testing (Figure 5) . TMP's A and B resulted in a nominal 3.8 mm thickness. TMP's C through E had a nominal 2 mm thickness.

An Instron Model TT-D floor model Universal Testing Machine was utilized for tensile testing. The test temperature was maintained by a Marshall Model 2232 clamshell furnace . Samples were placed in preheated grips and the assembly was quickly placed within the clamshell to reach equilibrium at the test temperature (300°C) within 30-40 minutes. Tensile testing was conducted using constant crosshead speeds providing nominal strain rates between 6.67×10^{-2} sec^{-1} and 6.67×10^{-5} sec^{-1}.

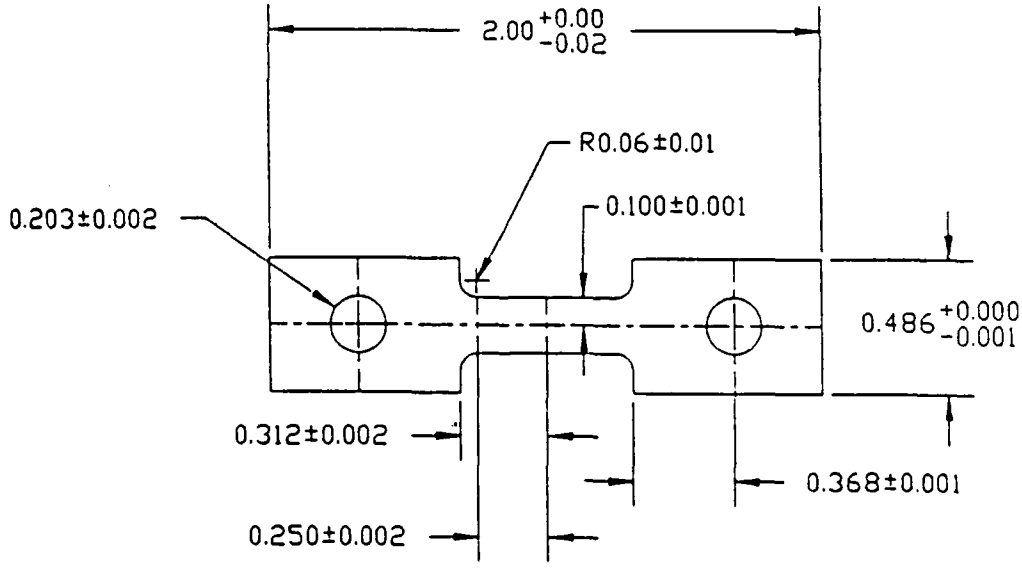

Figure 5. Tensile Test Specimen Design : dimensions and tolerances are in inches.

D. HARDNESS TESTING

Small coupons, 10mm x 15mm, were sectioned from the strips representing each TMP to examine the effect of subsequent annealing time on the hardness of the material. The coupons were placed in the Lindberg furnace that had been used for the solution treatment of the billets. The furnace was pre-heated to a temperature of 170°C to simulate the temperature of the preheated grips when installing tensile test samples. The furnace was then adjusted to 300°C. Heatup of the furnace thus approximated that of the Marshall clamshell employed in the tension testing (Figure 6) . The temperature of the samples was monitored with a thermocouple in contact with the coupons. When the coupon temperature reached 295°C (within 1% of the absolute test temperature) a timer was started to record the annealing interval. The intervals chosen were: 2, 5, 12.5, and 30 minutes. The coupons were water quenched to room temperature at the end of the tested interval.

Surface hardness readings were recorded using a Wilson Rockwell Hardness Tester on the Rockwell B scale. A minimum of five readings were taken and averaged per coupon. The coupons were then mounted on edge and polished using 6, 3, and 1 micron diamond paste and finally polish with cerium oxide.

Through thickness hardness readings were accomplished utilizing a Buehler Micromet Microhardness Tester. Vickers Hardness readings were obtained on the 300 gram scale.

E. DATA REDUCTION

True stress vs. true strain as well as engineering stress vs. engineering strain curves were reduced from Instron chart data recorded as a function of load vs. time. The data were compensated for the variation in constant crosshead speed such that stress vs. strain data are comparable. The correction is outlined by Lee and McNelley (Reference 14) .

True stress at a strain of $\varepsilon = 0.1$ vs. strain rate data were plotted on double logarithmic coordinates for each TMP condition to facilitate determination of the strain rate sensitivity coefficient m ($m = \partial \ln \sigma / \partial \ln \varepsilon$). The stress - strain data was also plotted at strains e = 0.02, 0.05, and 0.2 to assess the change of m with increasing strain.

F. OPTICAL MICROSCOPY

A Zeiss ICM-405 Optical Microscope was utilized for optical microscopy. Samples were mounted and initially polished with 3 micron diamond paste. Final polish was accomplished by electro-polishing in 33% Nitric acid and 67% Methanol maintained at a temperature of -24°C. The voltage (14VDC) was applied for 75 seconds.

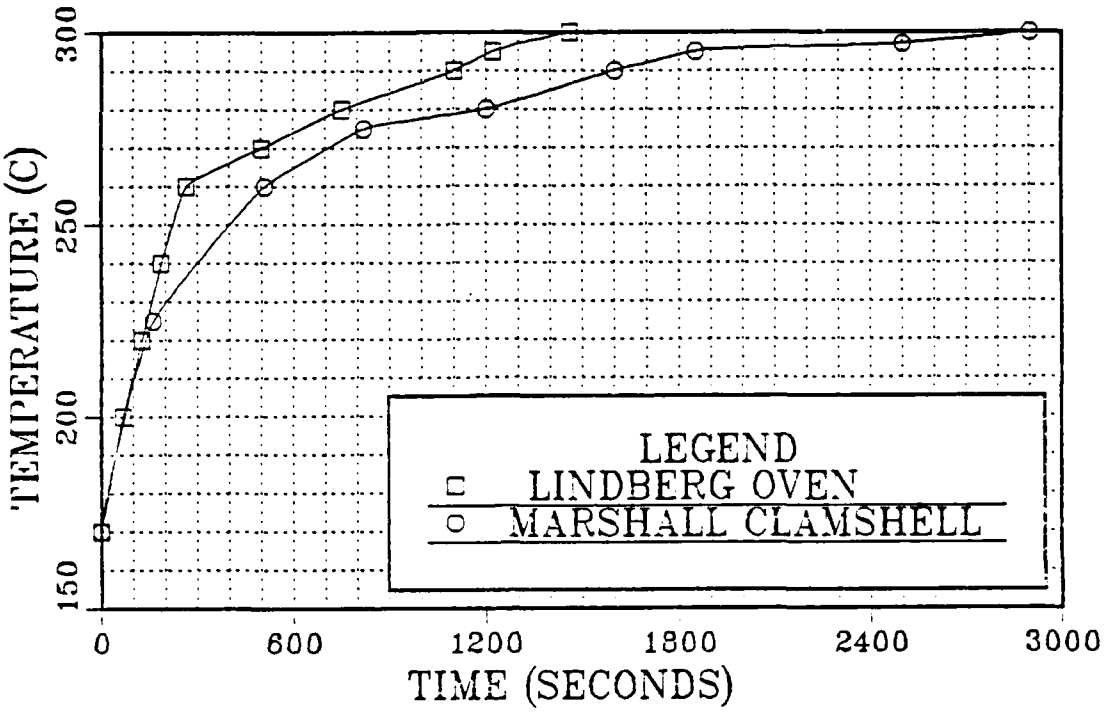

Figure 6. Furnace Heating Rates

IV. RESULTS AND DISCUSSION

Much of the previous work on superplastic Al alloys conducted at NPS has concentrated upon material processed through a "completed" TMP to $\varepsilon = 2.5$ (References 8, 15 - 17) . Material had been processed to this strain with different combinations of strain per pass and annealing interval between rolling passes (Reference 18) . Essentially all of the observations were recorded on finished material without regard to the development of the microstructure as a function of strain during processing. This research has examined in a consistent manner the evolution of properties and microstructure as the rolling strain increases. Two values of strain were chosen: the first, a total strain of 1.9, results from processing through ten rolling and annealing cycles; and the second, was a strain of 2.5 , a value employed in previous work and considered to represent a "finished" condition. The smaller value, 1.9, resulted in a sheet of sufficient length to ensure an adequate number of test samples, and yet a strain low enough to provide meaningful comparisons. Within each TMP, strict adherence to the rolling scheme developed by Chester (Reference 15) was used, and the annealing interval was varied between five and thirty minutes to attempt a correlation of the results obtained with a model for continuous recrystallization proposed by Hales, McNelley, and McQueen (Reference 10) .

The results will be presented by first looking at the data from each strain value to which the material was processed. Within each strain value, comparison of the effect of the annealing interval will be considered. Finally,

all of the results will be discussed in their relation to the proposed recrystallization model in the concluding section of this chapter.

A. RESULTS AT ε = 1.9

TMP's A and B represent materials rolled to a strain of 1.9 . This resulted in material roughly double the finished thickness of the previous work and the resulting material was just sufficient in rolled length to ensure adequate samples for experimentation. All mechanical test samples of each TMP were pulled to failure in tension (Figure 7) . Although the true stress - true strain curves are plotted to the point of sample failure, it is realized that the relation between true stress and true strain is not strictly valid after the onset of necking. Results compiled in Table 3, show a marginal superplastic response (peak ductility ~ 250% elongation) for TMP A .

TABLE 3. DUCTILITY (% ELONGATION) OF TMP A

Strain Rate	Ductility	σ @ ε = 0.1
6.67×10^{-2} s^{-1}	149	23514
1.67×10^{-2} s^{-1}	161	16819
6.67×10^{-3} s^{-1}	162	13083
6.67×10^{-4} s^{-1}	288	6035
1.67×10^{-4} s^{-1}	278	4204
6.67×10^{-5} s^{-1}	234	3150

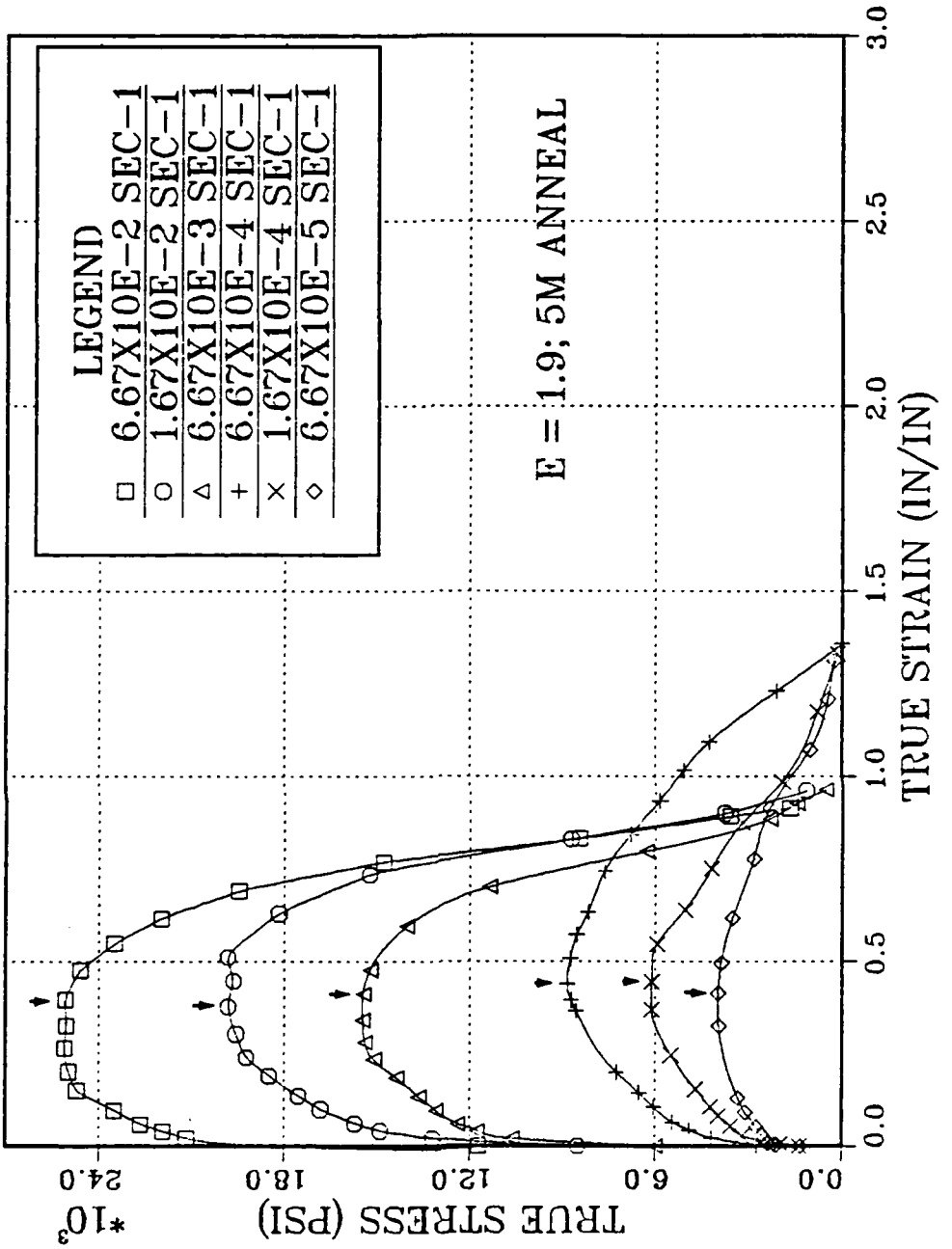

Figure 7. True Stress vs. True Strain for TMP A : arrow indicates point after which the relation between true stress - true strain is not strictly valid due to the onset of necking.

Comparing TMP B to A reveals some improvement in the superplastic properties as resulting from increased reheating interval (Table 4). The increase in resulting ductility associated with the longer reheating interval is seen at all strain rates with a maximum ductility attained of 500%(Figure 8) . Rolling with the longer annealing interval also softens the material while enhancing somewhat the superplastic response. The strain rate sensitivity coefficient, m, also reflects the improvement in superplastic response, increasing to 0.4 for TMP B (Figure 9) from a value of 0.3 for TMP A.

TABLE 4. DUCTILITY (% ELONGATION) OF TMP B

Strain Rate	Ductility	σ @ $\varepsilon = 0.1$
$6.67 \times 10^{-2}\ s^{-1}$	179	18743
$1.67 \times 10^{-2}\ s^{-1}$	279	11427
$6.67 \times 10^{-3}\ s^{-1}$	269	9489
$6.67 \times 10^{-4}\ s^{-1}$	300	3509
$1.67 \times 10^{-4}\ s^{-1}$	509	2594
$6.67 \times 10^{-5}\ s^{-1}$	317	2083

The microstructure of TMP A (Figure 10) in the as-rolled condition is seen to have no discernable grain size through optical microscopy. The distribution of the ß phase precipitates is banded. The as-rolled TMP B displays a more uniform distribution of coarser ß phase, although some banding is still evident.

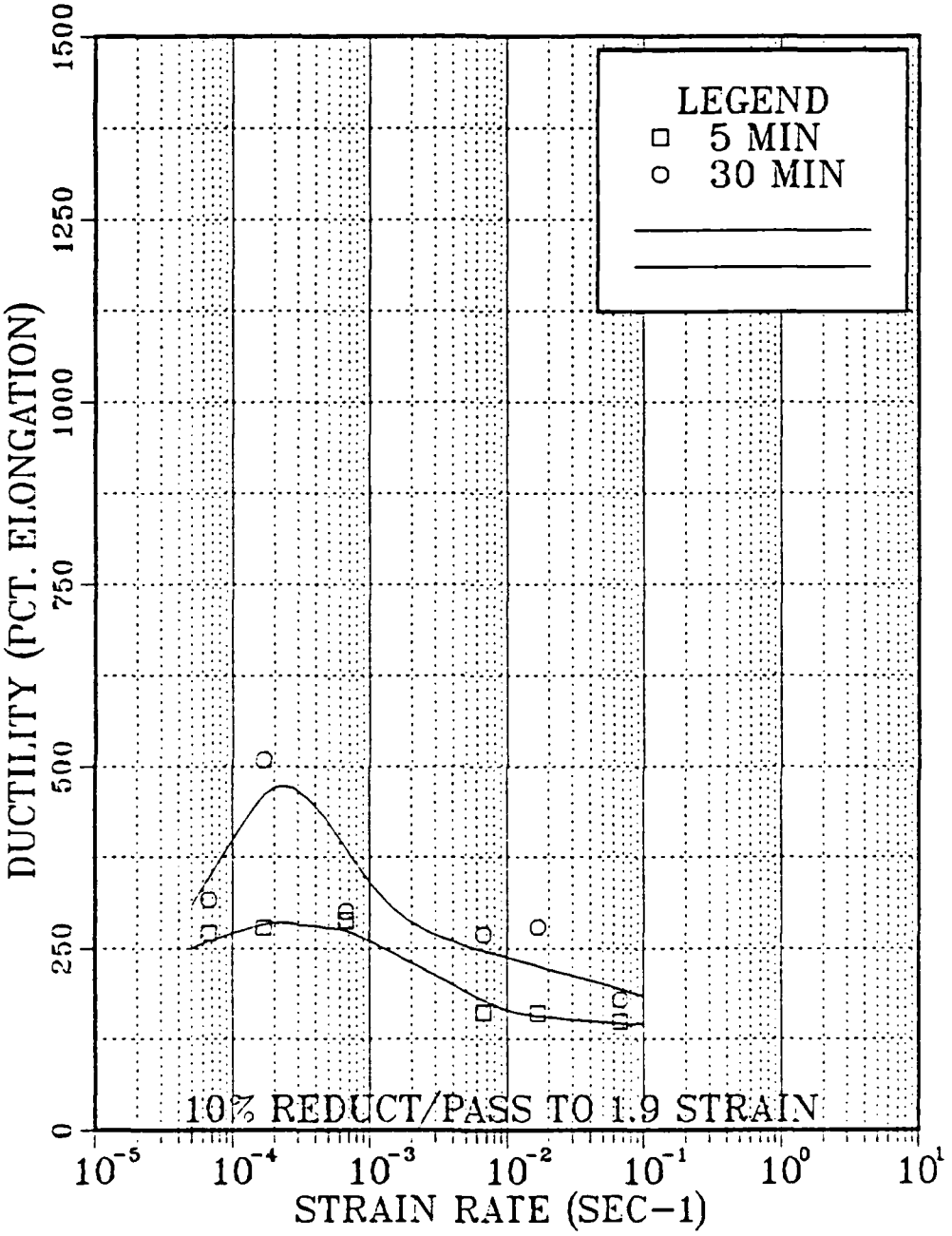

Figure 8. Ductility vs. Strain Rate for TMP's A and B

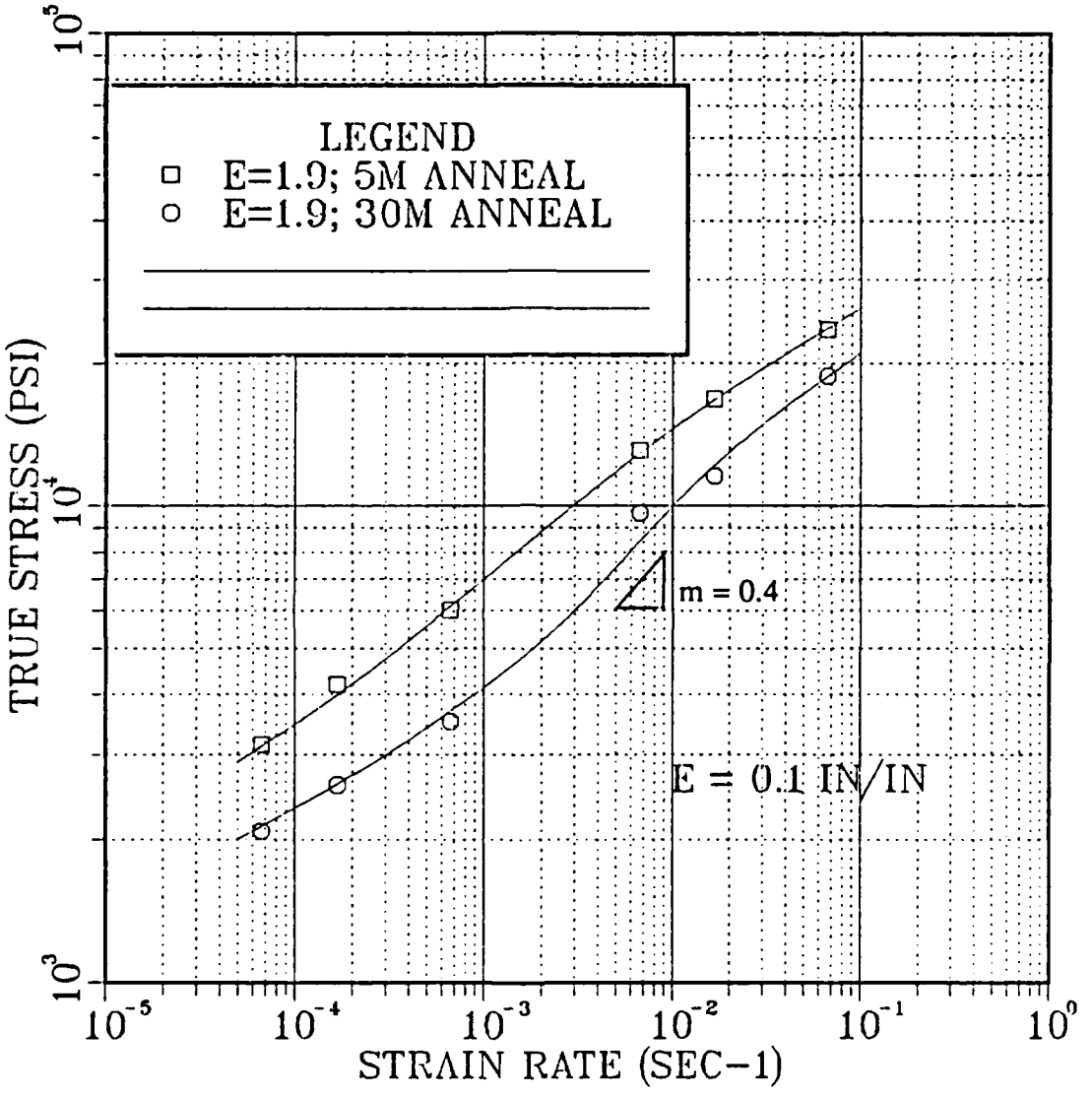

Figure 9. TMP A and B Strain Rate Sensitivity (m) : TMP A displays a maximum value of m = 0.3; TMP B has a maximum value m = 0.4

a)

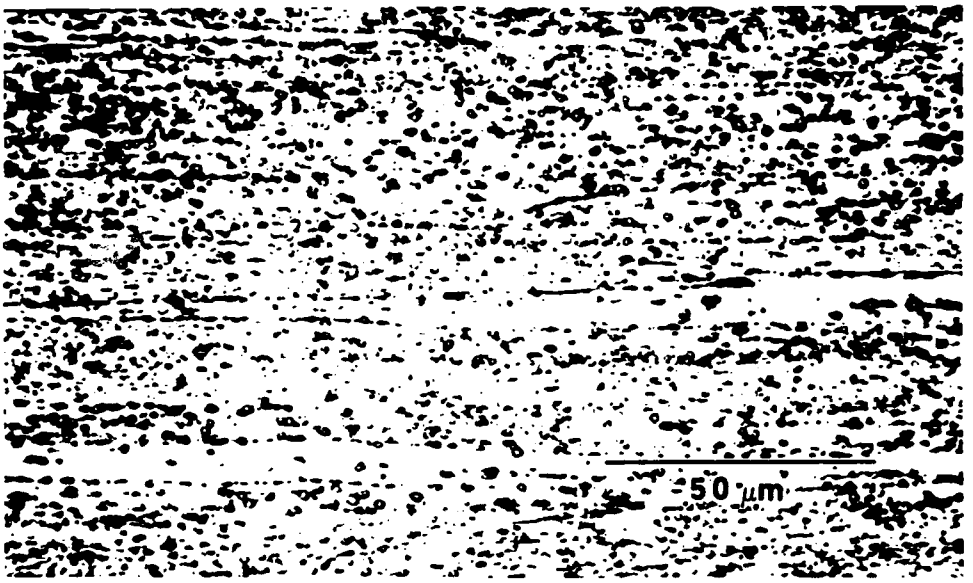

b)

Figure 10. TMP's A and B in As-Rolled Condition : a) cross-sectional view of TMP A showing irregular dispersion of ß phase precipitates, and layering of the material is evident (700x) b) TMP B showing improvement in the dispersion of ß in the microstructure (700x) .

B. RESULTS OF SUBSEQUENT ANNEALING

Between each pass through the rolling mill a reheating interval is utilized to facilitate recovery within the microstructure. In order to examine the effect on properties and microstructure that is imparted by the annealing interval, small samples were cut from the sheets representing each of the TMP's and then were annealed at 300°C for various intervals up to 30 minutes. Surface hardness and microhardness readings were taken on each of the samples. Six to eight readings using the Rockwell B scale were taken on each sample and averaged to obtain the surface hardness results. Though standard deviations up to 1.5 units on the B scale were observed, the results for TMP's A and B show that TMP B is initially harder than A (Figure 11) . This likely reflects the more uniform dispersion of the ß phase and a resulting higher dislocation density. However, within the first five minutes of annealing (where TMP A would be subjected to another rolling pass) TMP B has softened to a greater extent than TMP A, reflecting a structure that is better able to absorb and eliminate dislocations. Continued annealing to 30 minutes reduces the hardness further before TMP B would be rolled again.

Since deformation, especially at low values of strain, is not necessarily uniform throughout the thickness of the material, microhardness traverses through the thickness were performed. The traverse of TMP A (Figure 12) corresponds with the surface hardness values, showing an initial decrease in the hardness occurring in the first two minutes of annealing with little discernable decrease thereafter. This structure apparently cannot easily absorb and eliminate the dislocations introduced in the previous rolling pass. Lengthening the annealing interval displays more extensive softening in TMP B (Figure 13),

especially near the sample surface. Additionally, the decrease in hardness reflecting the development of the microstructure through the decrease in dislocation density at each annealing interval (2, 5, 12.5 & 30 min.), is more clearly discernable in TMP B.

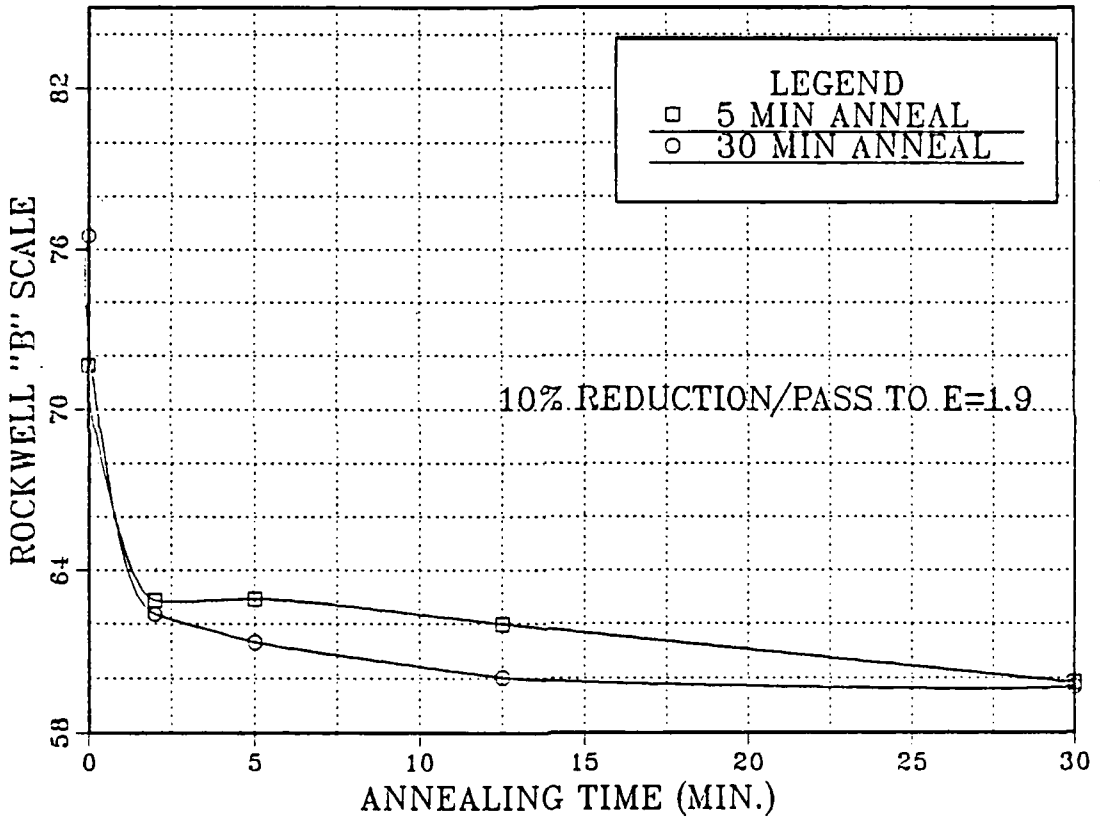

Figure 11. Surface Hardness for TMP's A and B : Rockwell B scale readings showing the decrease in hardness with longer annealing of TMP B.

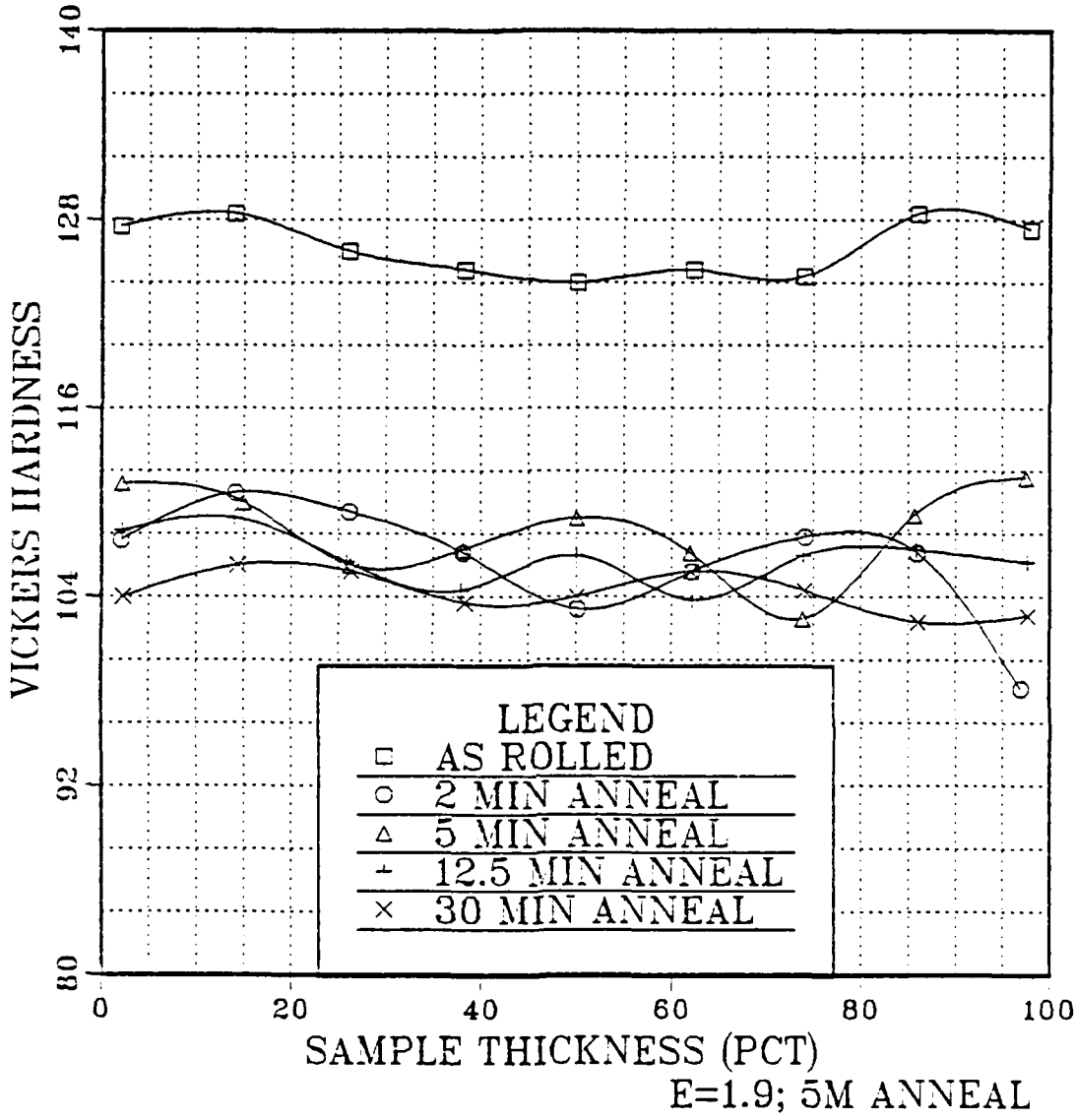

Figure 12. Microhardness Values for TMP A : readings taken through the sample cross-section showing hardness reduction in the first 2 minutes but little thereafter.

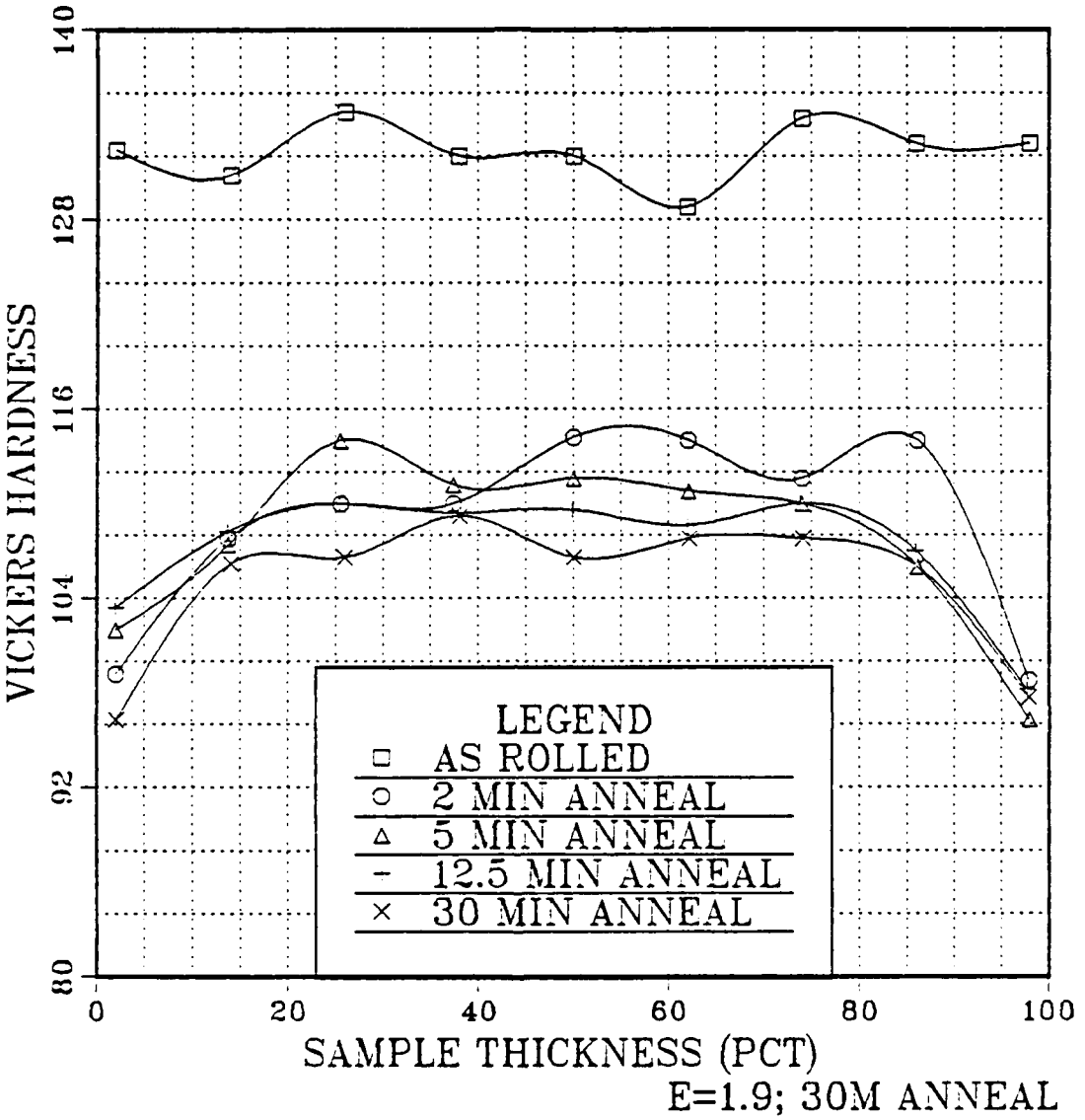

Figure 13. Microhardness Values for TMP B : note a small increase in hardness reduction over TMP A

C. RESULTS AT $\varepsilon = 2.5$

Further processing through two additional rolling passes increases the total accumulated strain to 2.5 . Although the number of additional rolling and annealing cycles is small, it represents approximately a 50% reduction in thickness compared to TMP's A and B. Viewing the microstructure of TMP's C-E, there is still no grain size evident through optical microscopy. TMP's A and C differ only in the total strain as the reheating interval was five minutes in both cases. The ß phase precipitate particles in TMP C (Figure 14) appear to be finer than previously seen in TMP A and the distribution is more uniform. This result may be due as much to the physical reduction of rolling, rather than a better dispersion per se. The banded appearance of TMP A is still observable in TMP C.

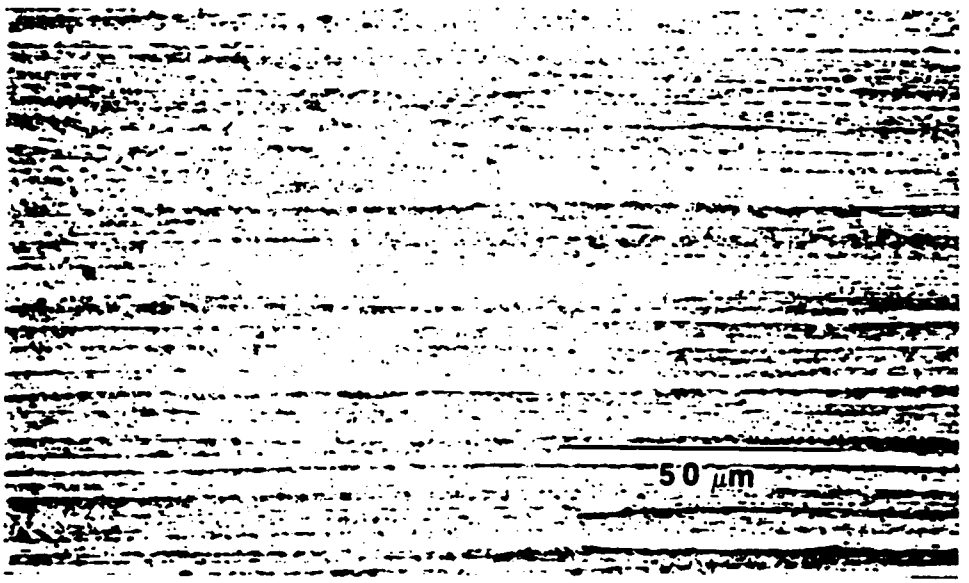

Figure 14. TMP C in As-Rolled Condition : cross-sectional view showing a fine structure of the ß phase precipitates (700x).

TMP D in the as-rolled condition (Figure 15) displays coarser ß phase precipitate particles resulting from the additional annealing time between passes, but still the dispersion shows some banding. The as-rolled condition of TMP E displays the most uniform dispersion of ß precipitates with no banding evident (Figure 16) . The microstructure of TMP E appears to be coarser than that of TMP C, reflecting the cumulative effect of the additional annealing time.

Figure 15. TMP D in As-Rolled Condition : cross-sectional view displaying the development of coarser ß phase precipitates with additional annealing (700x).

Figure 16. TMP E in As-Rolled Condition : cross-sectional view displaying the uniform dispersion of ß phase precipitates (700x).

The ductility obtained after rolling to a strain of 2.5 in TMP's C, D and E increases dramatically with the increase in the annealing interval between rolling passes (Table 5) . The short annealing period of five minutes in TMP C displays no improvement in ductility when compared to TMP A; however, there is a substantial improvement in ductility when the annealing interval becomes 30 minutes (TMP E verses TMP B) (Figure 17) .

TABLE 5. DUCTILITY (% ELONGATION) OF TMP'S C-E

A. TMP C

Strain Rate	Ductility	σ @ ε = 0.1
6.67×10^{-2} s^{-1}	138	24305
1.67×10^{-2} s^{-1}	166	18407
6.67×10^{-3} s^{-1}	163	12750
6.67×10^{-4} s^{-1}	241	6741
1.67×10^{-4} s^{-1}	270	4007
6.67×10^{-5} s^{-1}	169	3645

B. TMP D

Strain Rate	Ductility	σ @ ε = 0.1
6.67×10^{-2} s^{-1}	218	19975
1.67×10^{-2} s^{-1}	527	11622
6.67×10^{-3} s^{-1}	621	6304
6.67×10^{-4} s^{-1}	749	3050
1.67×10^{-4} s^{-1}	438	1832
6.67×10^{-5} s^{-1}	375	1425

TABLE 5. CONTINUED

C. TMP E

Strain Rate	Ductility	σ @ $\varepsilon = 0.1$
$6.67 \times 10^{-2}\ s^{-1}$	384	15922
$1.67 \times 10^{-2}\ s^{-1}$	744	10438
$6.67 \times 10^{-3}\ s^{-1}$	831	6150
$1.67 \times 10^{-3}\ s^{-1}$	1008	3061
$6.67 \times 10^{-4}\ s^{-1}$	1118	2929
$1.67 \times 10^{-4}\ s^{-1}$	623	1707
$6.67 \times 10^{-5}\ s^{-1}$	416	1394

Given sufficient recovery time the additional dislocations introduced by further straining apparently migrate to form a refined structure with a sufficient misorientation between the grains to permit extensive superplastic deformation. As the annealing interval increases to 12.5 minutes or more, the strain rate sensitivity coefficient increases to 0.5 for both TMP D and E (Figure 18) .

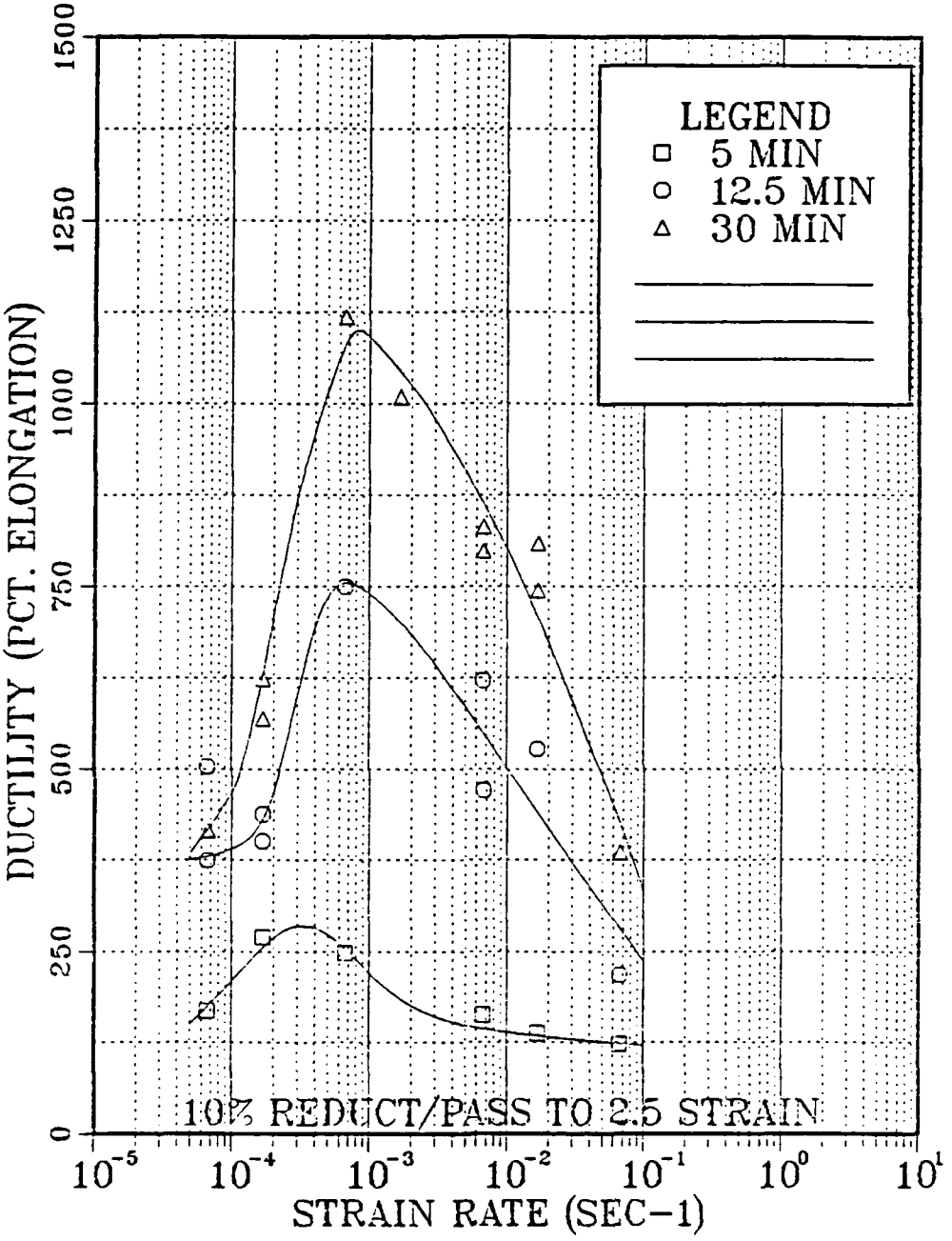

Figure 17. Ductility vs. Strain Rate for TMP's C Through E : showing the wide range of superplasticity with strain rate for TMP's D and E .

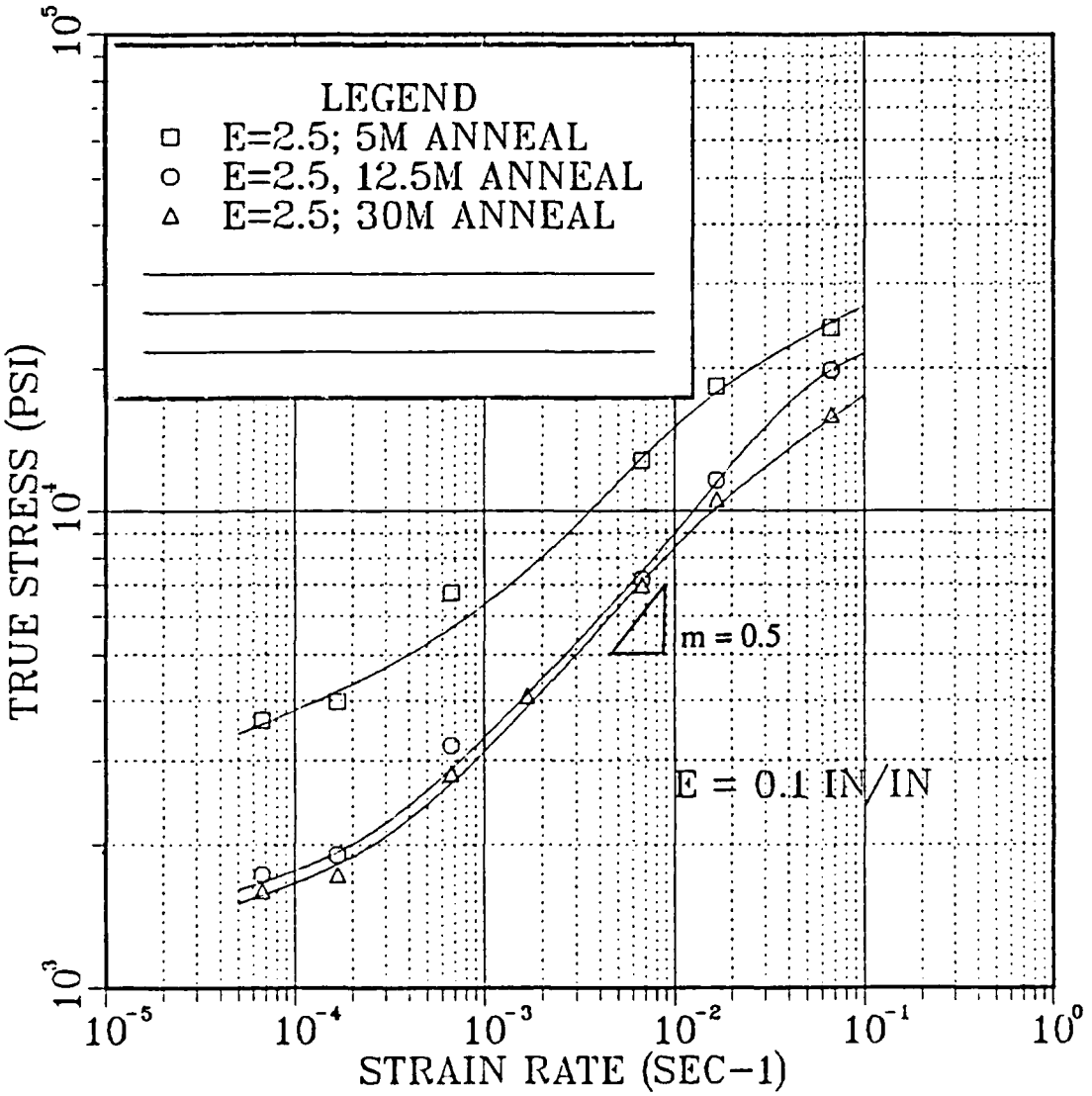

Figure 18. TMP's C - E Strain Rate Sensitivity (m) : maximum value of m for TMP C remains about 0.3 while maximum value for both TMP D and E increases to nearly 0.5 .

To observe the results of subsequent annealing on the "finished" material rolled to a strain of 2.5, and to observe the effect of annealing that occurs during the heat-up of tensile test samples, specimens were cut from TMP's C - E and heated in a similar manner to those of the earlier tests at 1.9 strain. The results of surface hardness readings (Figure 19) correlate with those at a strain of 1.9 (Figure 11) . TMP's C-E show an increase in hardness in the as-rolled condition from TMP's A and B due to the accumulation of dislocations induced by rolling to the higher strain. TMP C displays an increase from 72 (ε = 1.9) to 82 (ε = 2.5) on the Rockwell B scale while TMP E increases from 77 to 83 over the same increase in strain. This may reflect the accumulation of dislocations within the grains of the TMP C material which is subject to a short reheating interval as opposed to the more fully developed boundary structure of TMP E which is able to absorb more of the dislocations during reheating. Further, both materials (TMP's B and E) which use long reheating intervals anneal to the same value (60) on the Rockwell scale, displaying a structure which is more fully developed or near equilibrium. TMP E still softens faster in the first five minutes than TMP C, a similar result as observed in comparison of TMP B to TMP A, again demonstrating the ability of the microstructure to absorb dislocations more readily. The total change in dislocation density in TMP E is likely greater than that in TMP C as shown by the decrease in the Rockwell scale of 23 points for TMP E verses only 15 points for TMP C over their respective annealing intervals.

The microhardness traverses show similar results (Figures 20 - 22). Longer annealing displays a significant softening in the processed material -- TMP C softens by 20 points on the Vickers Hardness Scale in a five minute anneal, while

TMP E's hardness is reduced 30 points in a 30 minute annealing interval. This suggests that the short annealing intervals do not allow a complete transformation to a stable substructure and leave residual dislocations within the grains. Further evidence of a more complete recovery process can be seen in the uniformity of the Microhardness traverses of TMP E compared to TMP C .

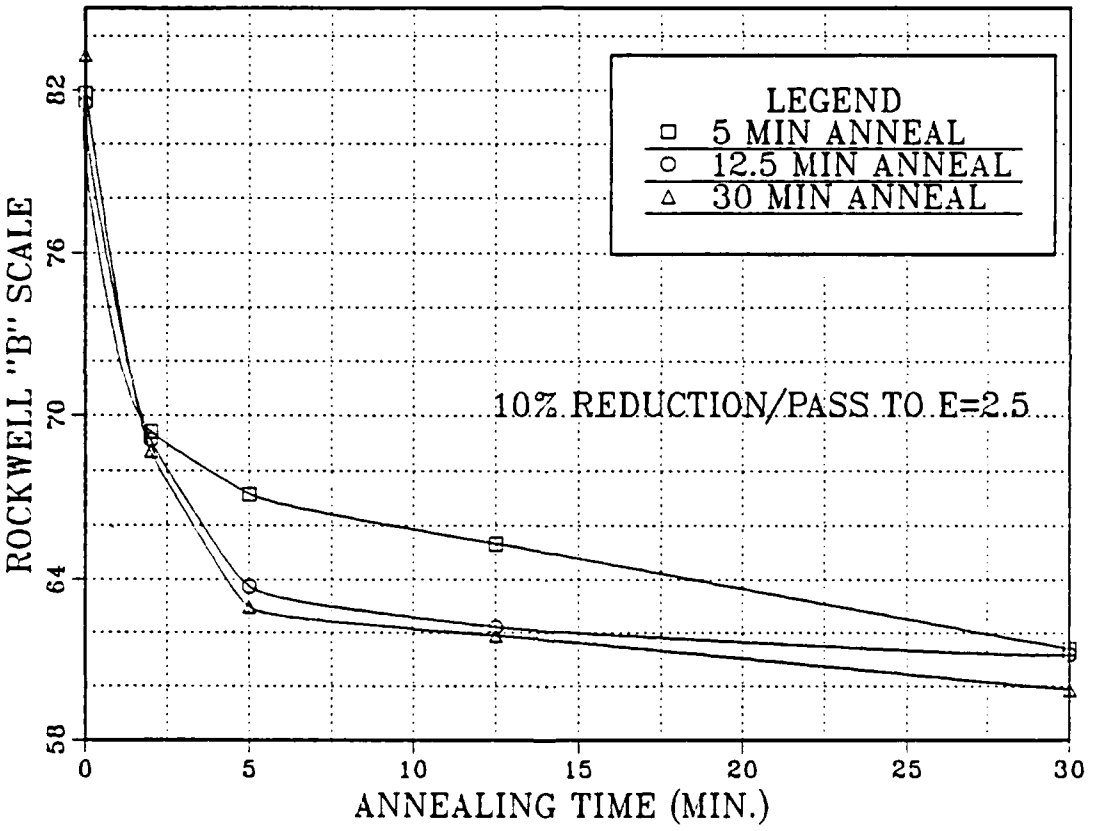

Figure 19. Rockwell Hardness for TMP's C Through E : further evidence of the increased recovery by lengthening the annealing interval .

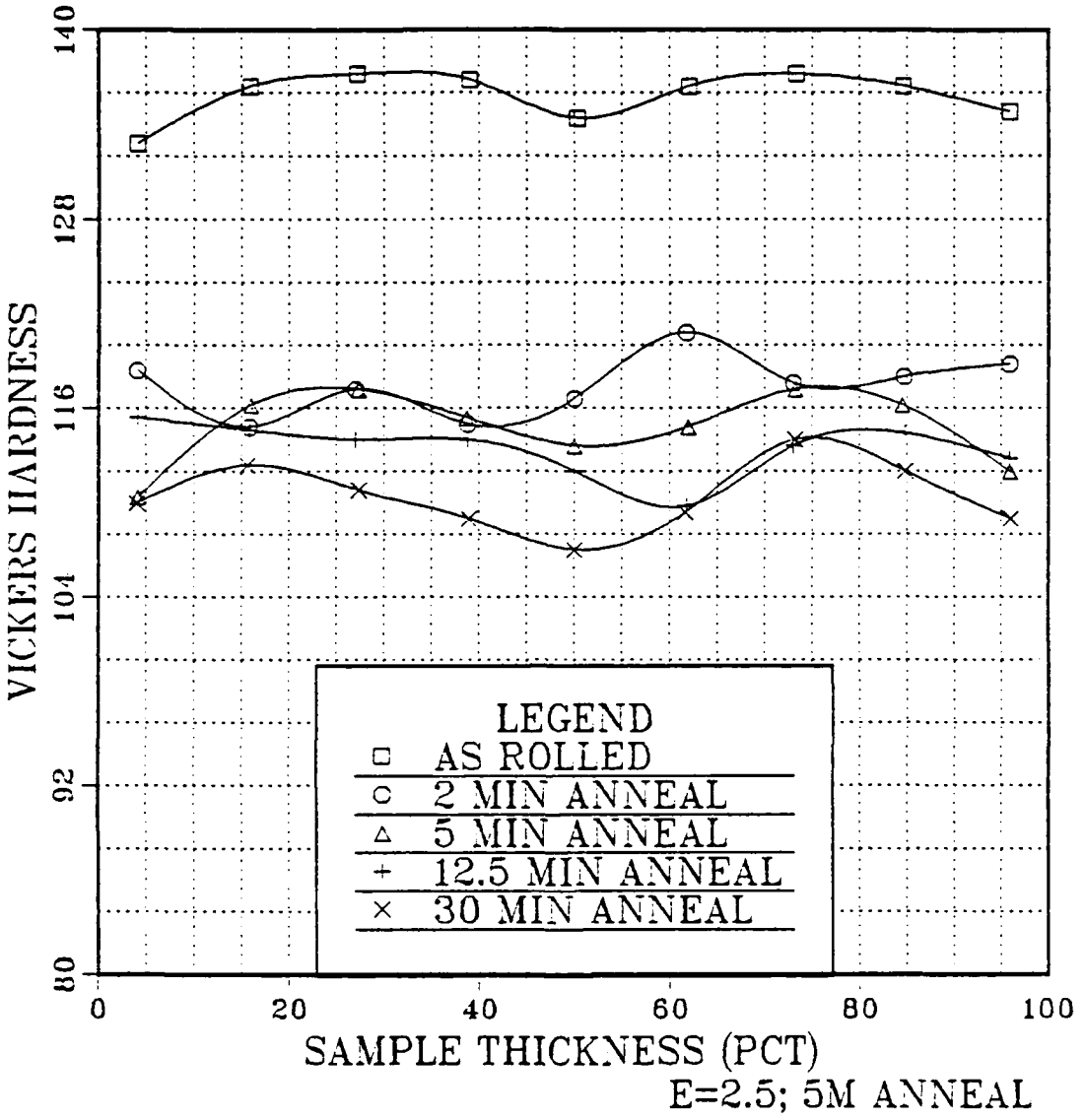

Figure 20. Microhardness Values for TMP C : the as rolled hardness has increased over TMP A reflecting a higher dislocation density with further straining, however the relative softening with annealing has not increased indicating insufficient time for well structured subgrain boundaries to form .

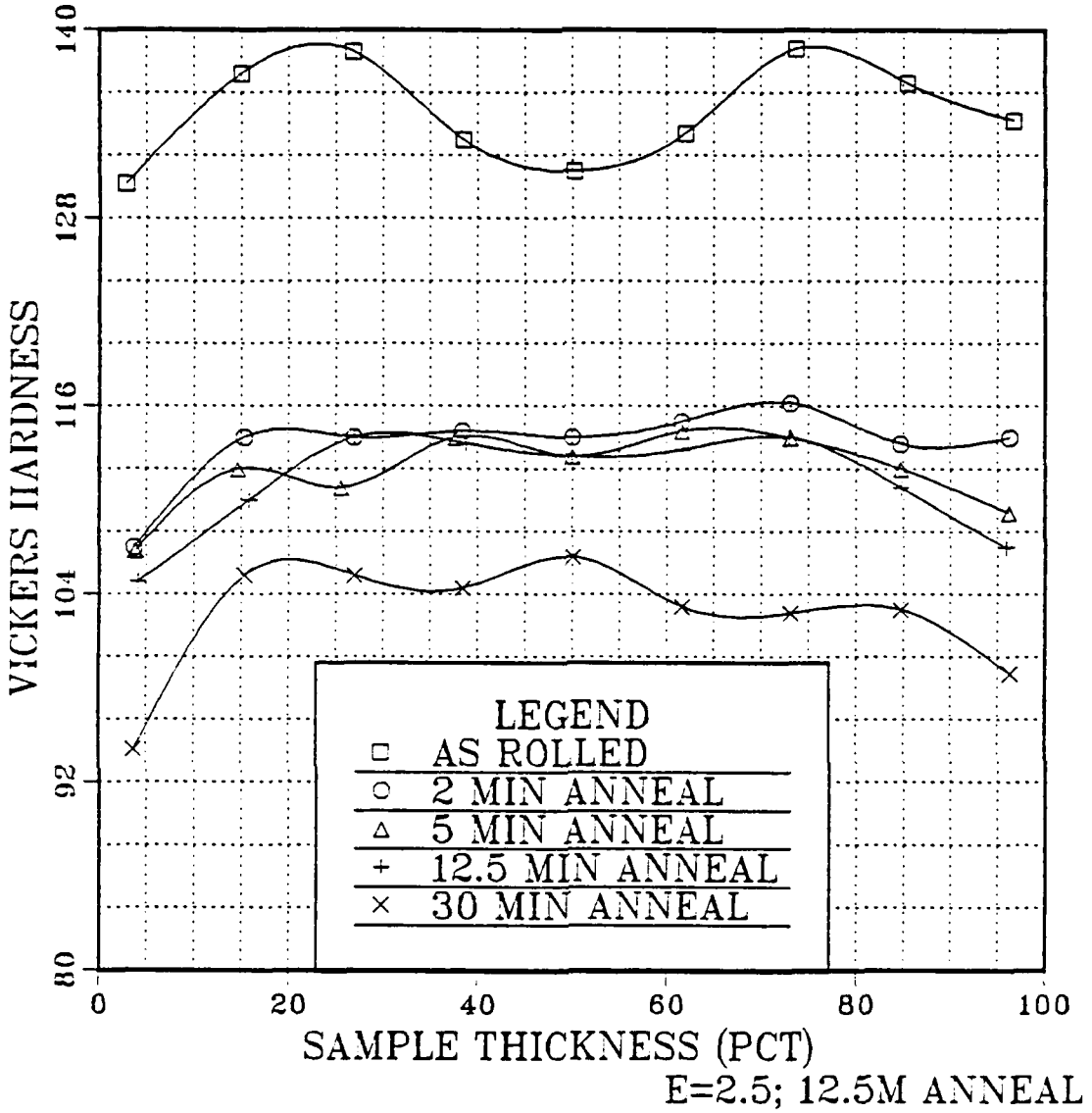

Figure 21. Microhardness Values for TMP D : the as rolled condition is not as uniform in hardness, perhaps indicating an incomplete transformation to a more well structured boundary condition. There is a noticeable reduction in hardness between the 12.5 min. and 30 min. annealing interval .

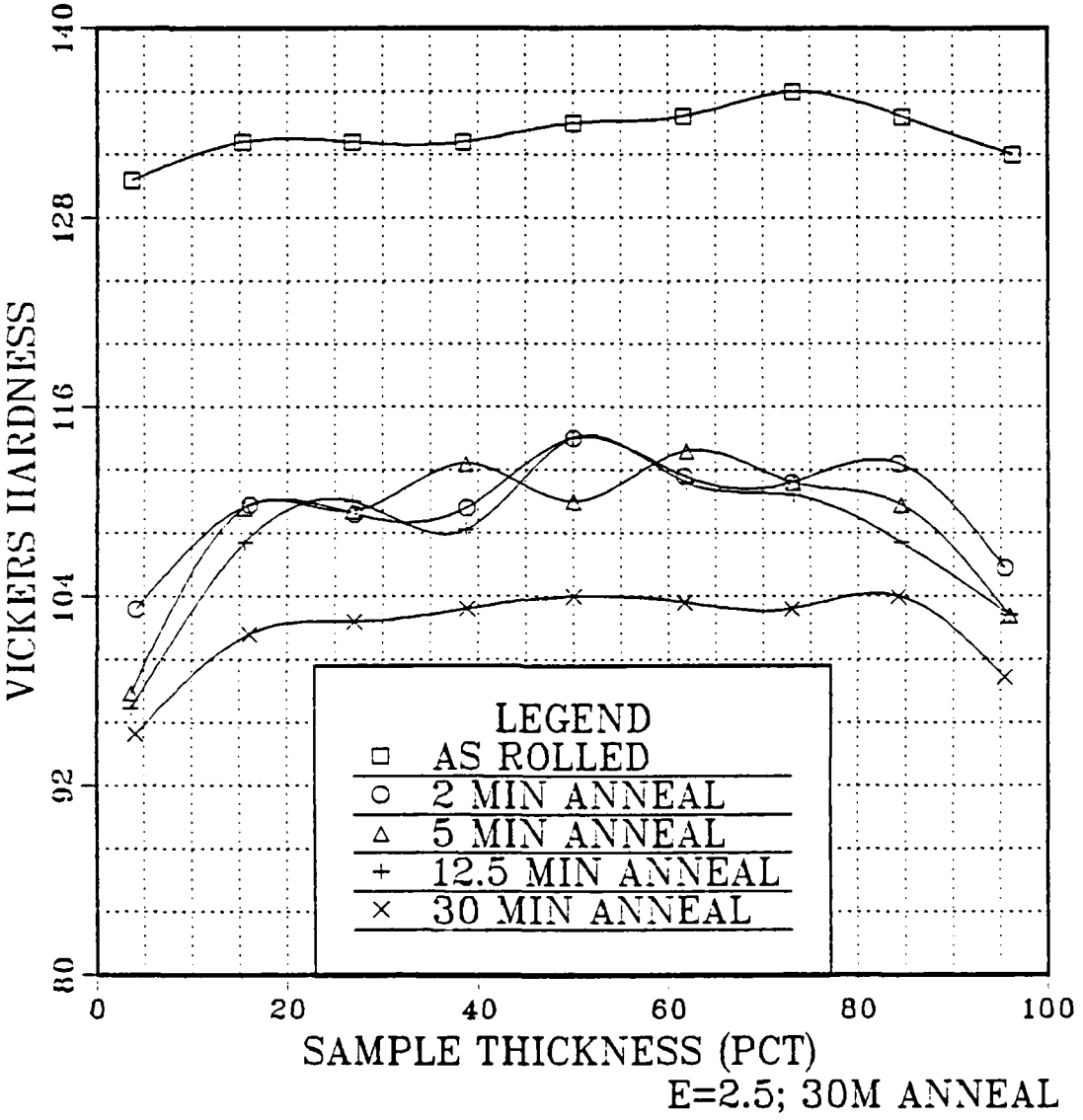

Figure 22. Microhardness Values for TMP E : note the uniformity of the as rolled and 30 min. annealed conditions, however the hardness of the 30 min. interval in E is not appreciably less than in TMP D giving credence to D's high degree of superplasticity.

D. SUMMARY

It has been proposed (Reference 10) that a balance between conditions of deformation and recovery allows the progressive absorption of dislocations into an evolving substructure during the sequence of deformation and annealing cycles. Comparison of TMP's A and B, which have accumulated a total strain equal to 1.9, to TMP's C through E which were strained to 2.5, show the latter to have a more uniform dispersion of ß phase precipitates. This would allow development of a more refined and homogeneous boundary structure necessary to support superplastic response . The density of dislocations generated in each successive rolling pass is dependent upon the strain and strain rate per pass, and both of these increase due to the fixed reduction schedule employed. Thus the resultant subgrain size that evolves during subsequent annealing becomes smaller and the ß phase precipitates that were initially at the nodes of the substructure before the rolling pass may now have a spacing greater than the subgrain size (Reference 10) .

The lesser number of rolling passes in TMP's A and B result in subgrains that are not pinned by ß phase precipitates. These subgrains would coalesce resulting in more highly misoriented boundaries in the vicinity of the ß particles, and as rolling strain increases the number of these boundaries increase and capacity for superplastic deformation is enhanced.

Recovery during the annealing interval shows an even greater impact on the ability to achieve superplastic deformation. The short reheating interval in either TMP's A and C results in a minimal superplastic response. With a short interval between each rolling pass there is likely insufficient time for a substructure to develop. Microscopy of TMP A after annealing for five

minutes reveals that the dispersion of ß phase precipitates remains non-uniform (Figure 23) thus affording less stability to the boundary structure. With further rolling to a strain of 2.5 the dispersion of ß particles becomes finer and more uniform but the substructure that forms apparently remains fine in size with boundaries of small misorientation. Since there is less time for the dislocations introduced during the rolling pass to migrate to the subgrain boundaries a higher dislocation density remains in the interior of the grains and this results in retention of a finer structure of lower misorientation angles between the grains (Figure 24) (Reference 10).

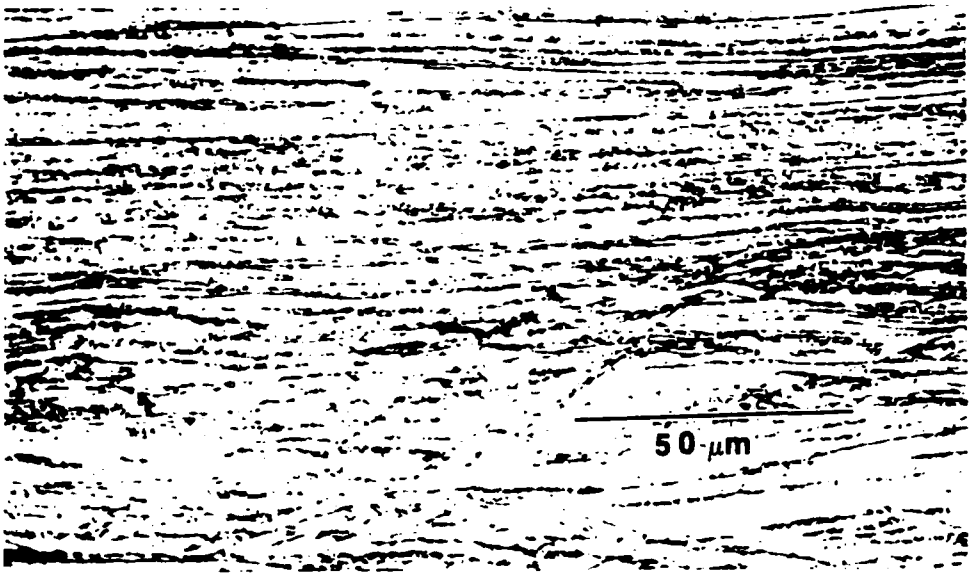

Figure 23. TMP A After Annealing for Five Minutes : still displaying a non-homogeneous dispersion of the ß phase; appears again similar to an extruded material (700x)

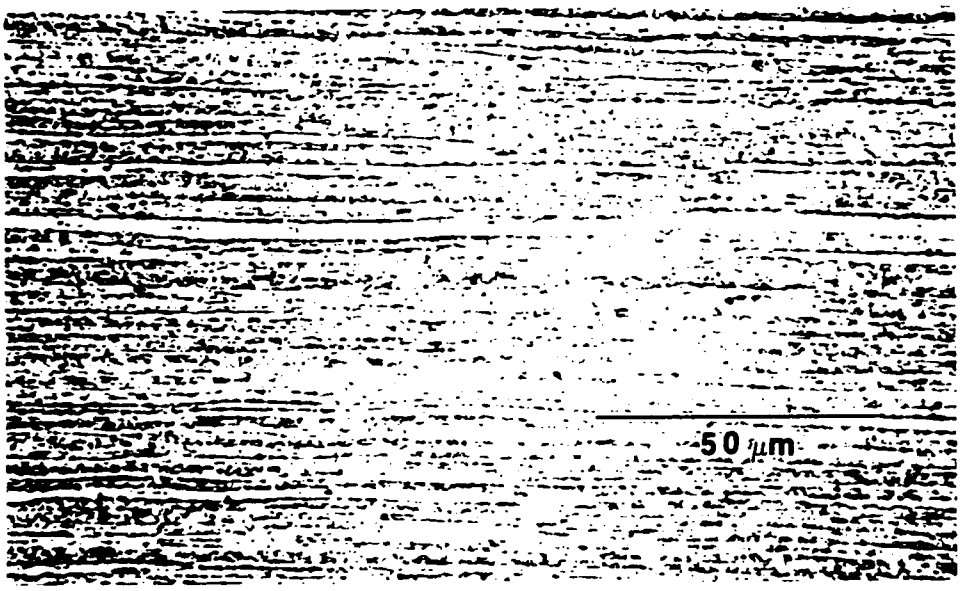

Figure 24. TMP C After Annealing for Five Minutes : displays little coarsening and the layered structure is still quite evident. The microstructure still does not support a superplastic response (700x) .

The increase in the annealing interval means a corresponding increase in the total time at temperature, thus allowing an increase in the total ß phase precipitation and completion of the precipitation will occur at a lower value of strain. Thus the spacing between the precipitates is small at an earlier stage of processing and the evolving substructure is likely more stable. As the recovery time increases from five to 12.5 to 30 minutes the time at temperature increases to six hours, the ß precipitates coarsen slightly and the dispersion becomes much more uniform. Comparison of the microstructure of TMP B at a strain of 1.9 (Figure 25) to that of TMP D at a strain of 2.5 shows little difference between

them. The structure of the material processed using a 12.5 minute anneal is somewhat finer than that with the 30 minute anneal but the banding of the dispersion is still observable (Figure 26) . TMP E again displays the most fully developed structure (Figure 27) .

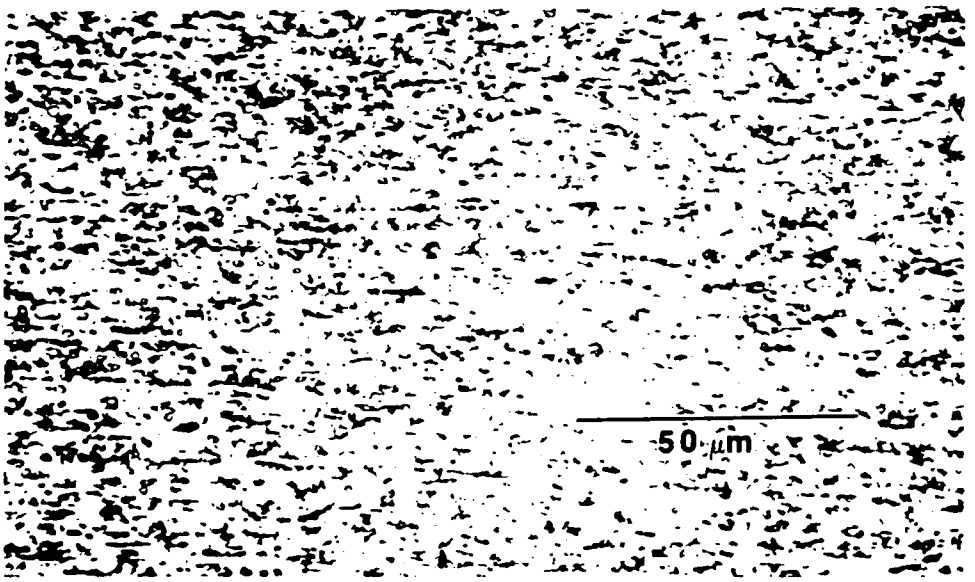

Figure 25. TMP B After a 30 Minute Anneal : shows some coarsening over the as-rolled condition but dispersion is not completely uniform (700x) .

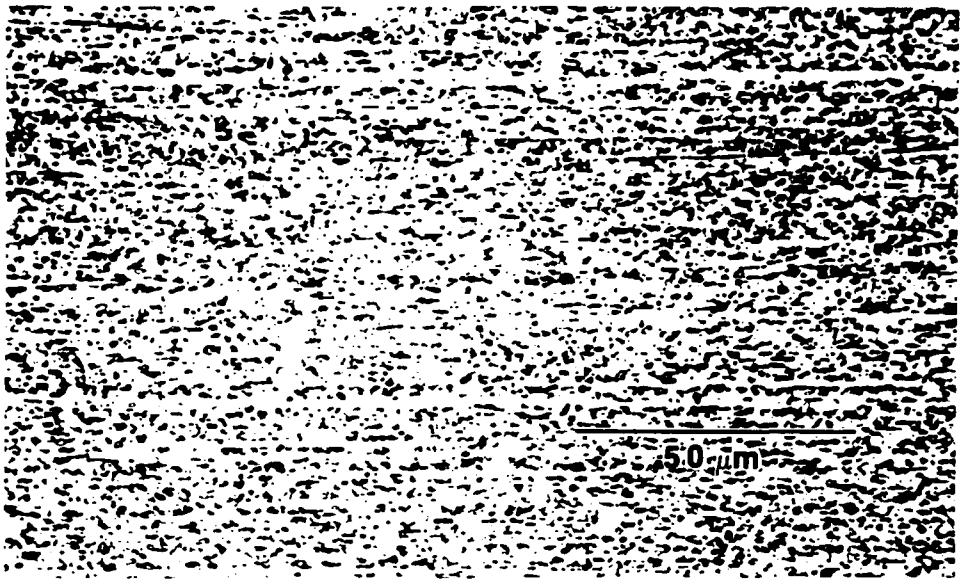

Figure 26. TMP D After a 12.5 Minute Anneal : the ß phase precipitates are finer than TMP B but are more evenly distributed (700x) .

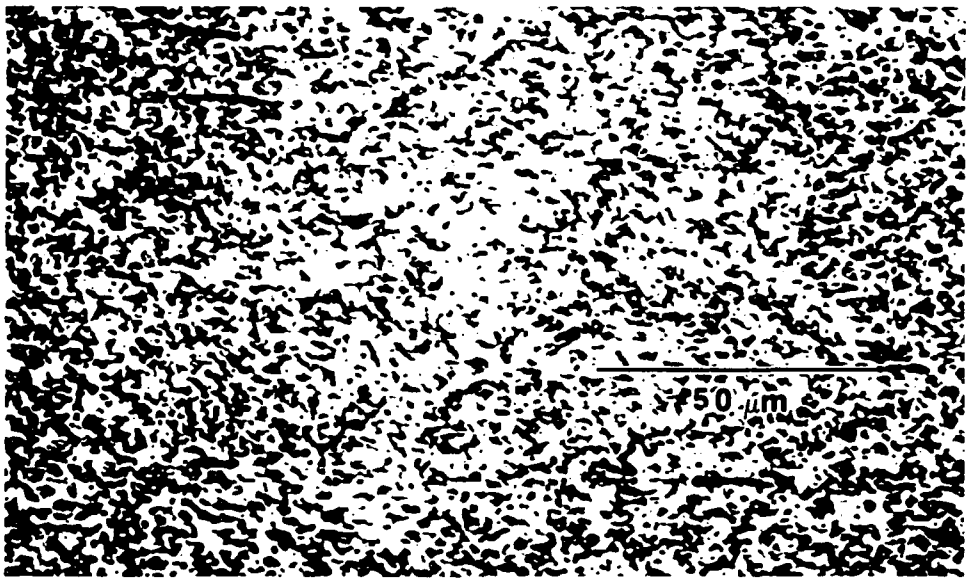

Figure 27. TMP E After a 30 Minute Anneal : shows complete dispersion of the ß phase (700x) .

In previous work (References 8 and 19), transmission electron microscopy (TEM) has been conducted to ascertain the boundary character (especially the boundary misorientation) in the development of superplastic behavior. The essential result of this previous work is shown in Figure 28. The figure shows TMP 6 (similar to TMP E), which utilizes a long reheating interval in processing material to a strain of 2.5, displaying a spectrum of misorientation angles where more than 70% of the grain boundaries have misorientation > 15^{o}. The opposite is true when only a short reheating interval is employed as shown in TMP 2 (similar to TMP C) where > 70% of the boundaries are low angle (< 15^{o}) in character. The other TMP shown in the figure (TMP 3) utilized smaller reductions per pass in processing. Weinberg (Reference 20; p. 808) has shown that grain boundary sliding, which is essential to superplastic deformation, can occur at misorientation angles as low as 7^{o}. Thus increasing the reheating interval allows the requisite microstructure to form earlier in the TMP. Also, this allows the generation of more dislocations in subsequent cycles which are able in turn to recover to evolving boundaries, increasing their misorientation sufficiently to support superplastic deformation.

The focus of this research was to investigate the effects of strain and annealing interval in achieving superplastic deformation. A TMP which follows a rigid schedule of increasing strain rate per pass with sufficient annealing between passes will produce a superplastic response in Al-9.89Mg-0.09Zr at 300^{o}C . Strong correlation with the results of this research and the model for superplastic response proposed by Hales, McNelley and McQueen (Reference 10) exists.

Further investigation is needed in the area of TEM to see if grain size and substructure boundary misorientation correspond to those of earlier work. Additionally, investigation at even longer annealing intervals and tension testing at rates beyond this research should be conducted to gain a broader spectrum of material response.

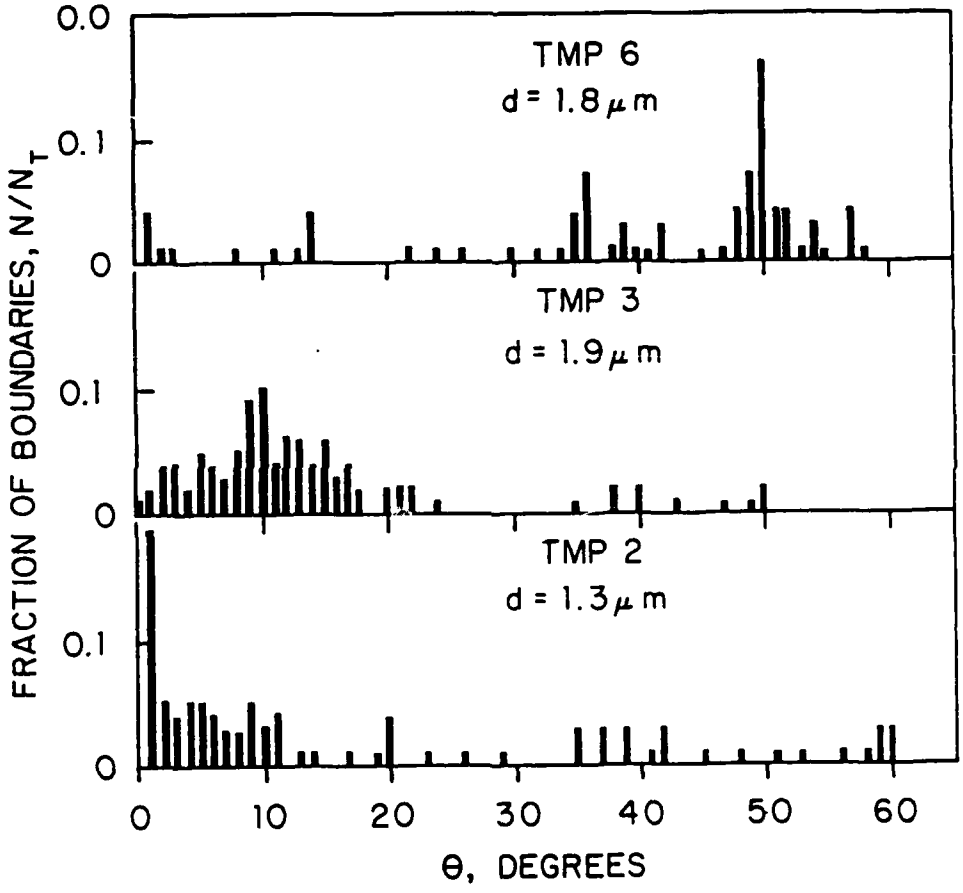

Figure 28. Spectrum of Grain Boundary Misorientation Angle, θ : previous work at NPS shows the variation in angle resulting from various TMP's - TMP 6 is a 30 min rolling / annealing cycle; TMP 2 is a 5 min. cycle. Note the large number of low angle boundaries in 2 vs. 6 (Reference 19, reprinted by permission).

V. CONCLUSIONS

1. Al-9.89Mg-0.09Zr is capable of superplastic deformation at 300°C to a ductility in excess of 1000% after thermomechanical processing at 300°C to a strain of 2.5 and with sufficient recovery time between rolling passes.

2. The development of a microstructure capable of supporting 300°C superplastic response is dependent on a series of deformation and annealing cycles. There was a substantial improvement in ductility between processing at 300°C to a strain of 1.9 and to 2.5 .

3. The length of the annealing interval is critical to the recovery in the microstructure necessary to create boundaries of sufficient misorientation angle to allow grain boundary sliding. A five minute reheating interval at 300°C is too short to provide any ductility improvement in this alloy.

4. Strain rate sensitivity coefficient, m, was approximately equal to 0.5 over a range of strain rates from 6.67×10^{-4} sec^{-1} to 1.67×10^{-2} sec^{-1} for a TMP with a long annealing interval for each rolling cycle (12.5 to 30 minutes) .

VI. RECOMMENDATIONS FOR FURTHER STUDY

1. Investigate Scanning Electron Microscopy (SEM) and Transmission Electron Microscopy (TEM) for further identification of grain size and a measure of grain boundary angle misorientation.

2. Investigate still longer annealing intervals (> 30 min.) to determine a maximum recovery time beyond which there is no improvement in the superplastic response.

3. Investigate tensile testing beyond the range of strain rates utilized in this research to define the ductility vs. strain rate curves further.

APPENDIX A. TRUE STRESS VS. TRUE STRAIN CURVES

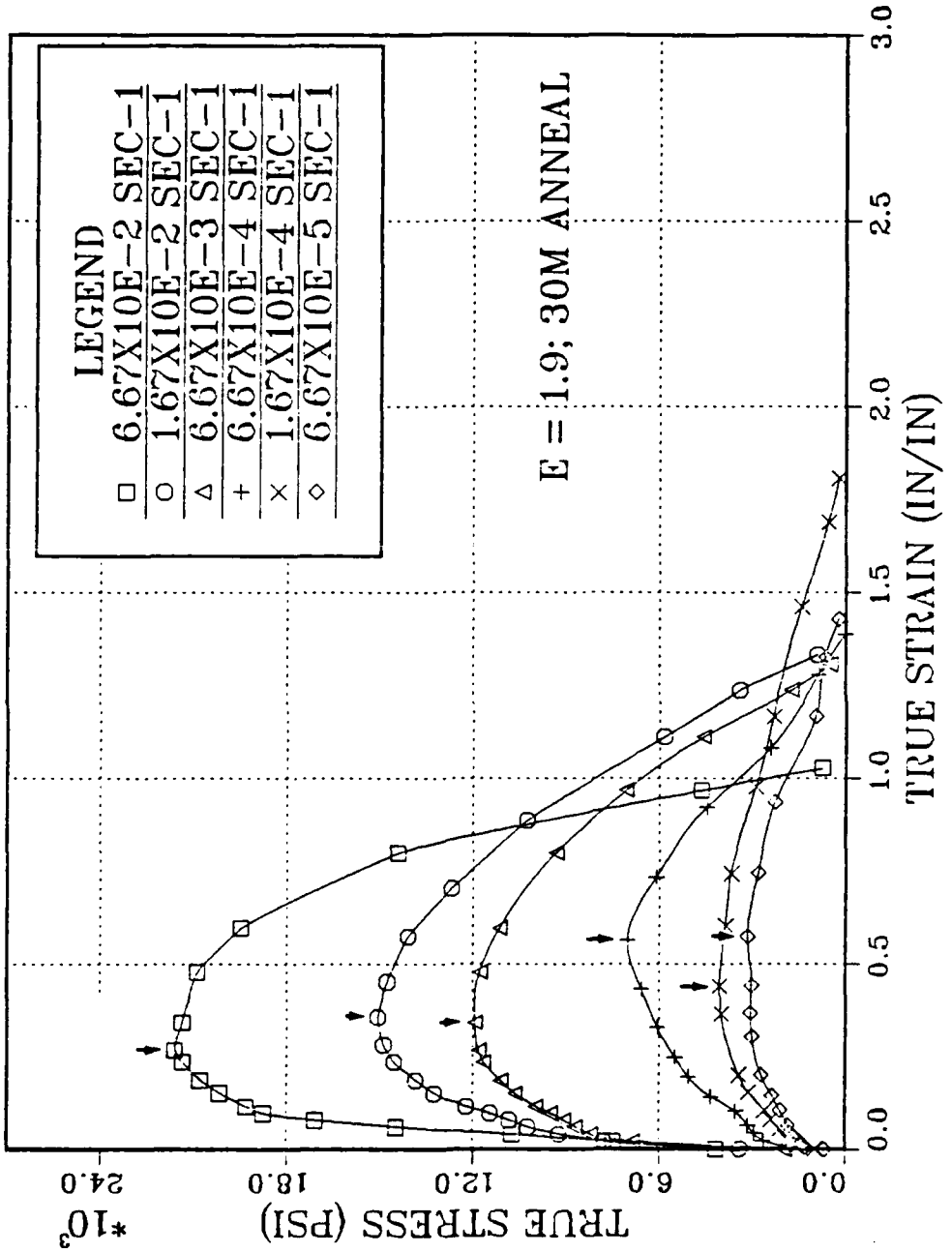

Figure 29. Stress Strain Curve for TMP B : arrow indicates point after which the relation between true stress - true strain is not strictly valid due to the onset of necking.

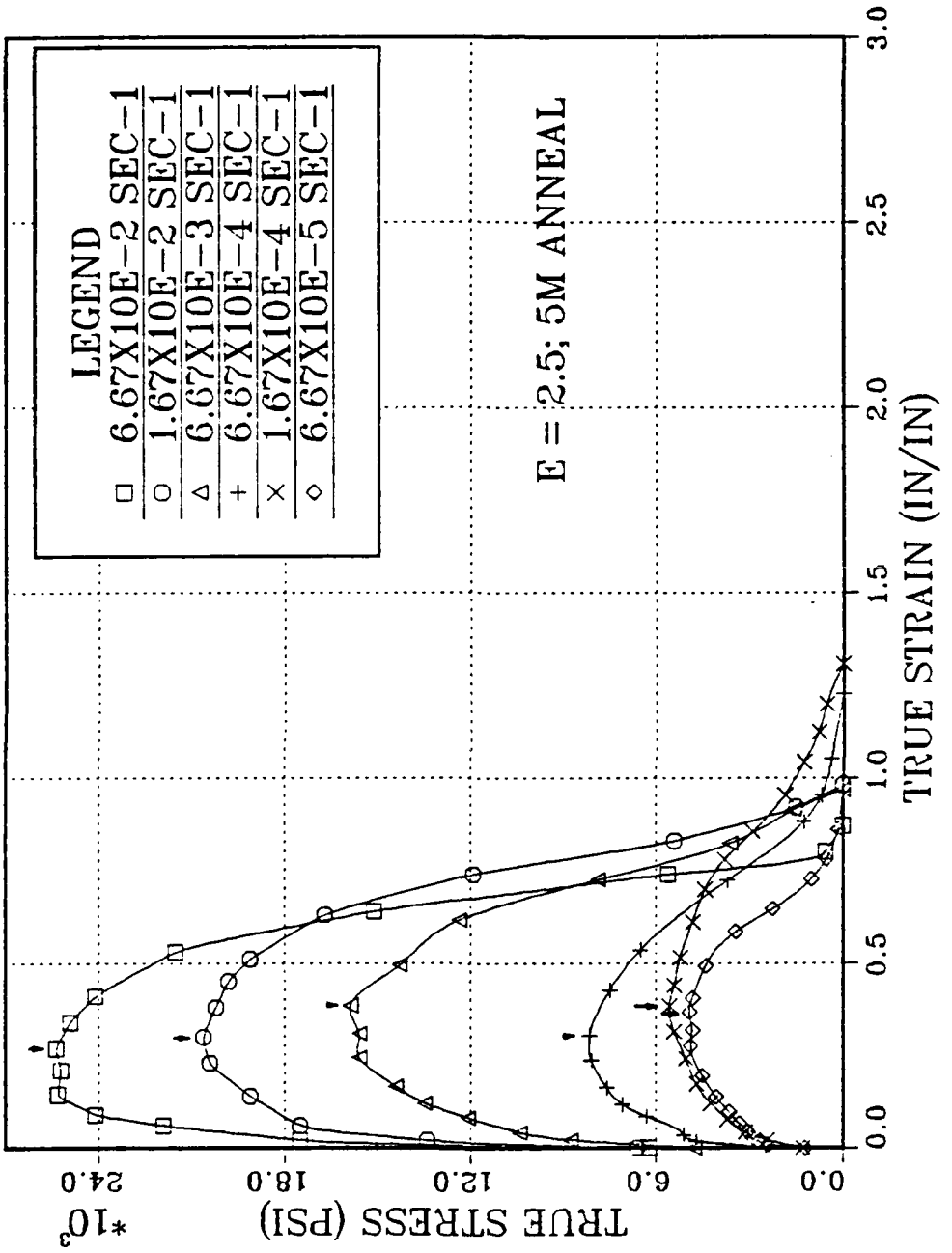

Figure 30. Stress Strain Curve for TMP C : arrow indicates point after which the relation between true stress - true strain is not strictly valid due to the onset of necking.

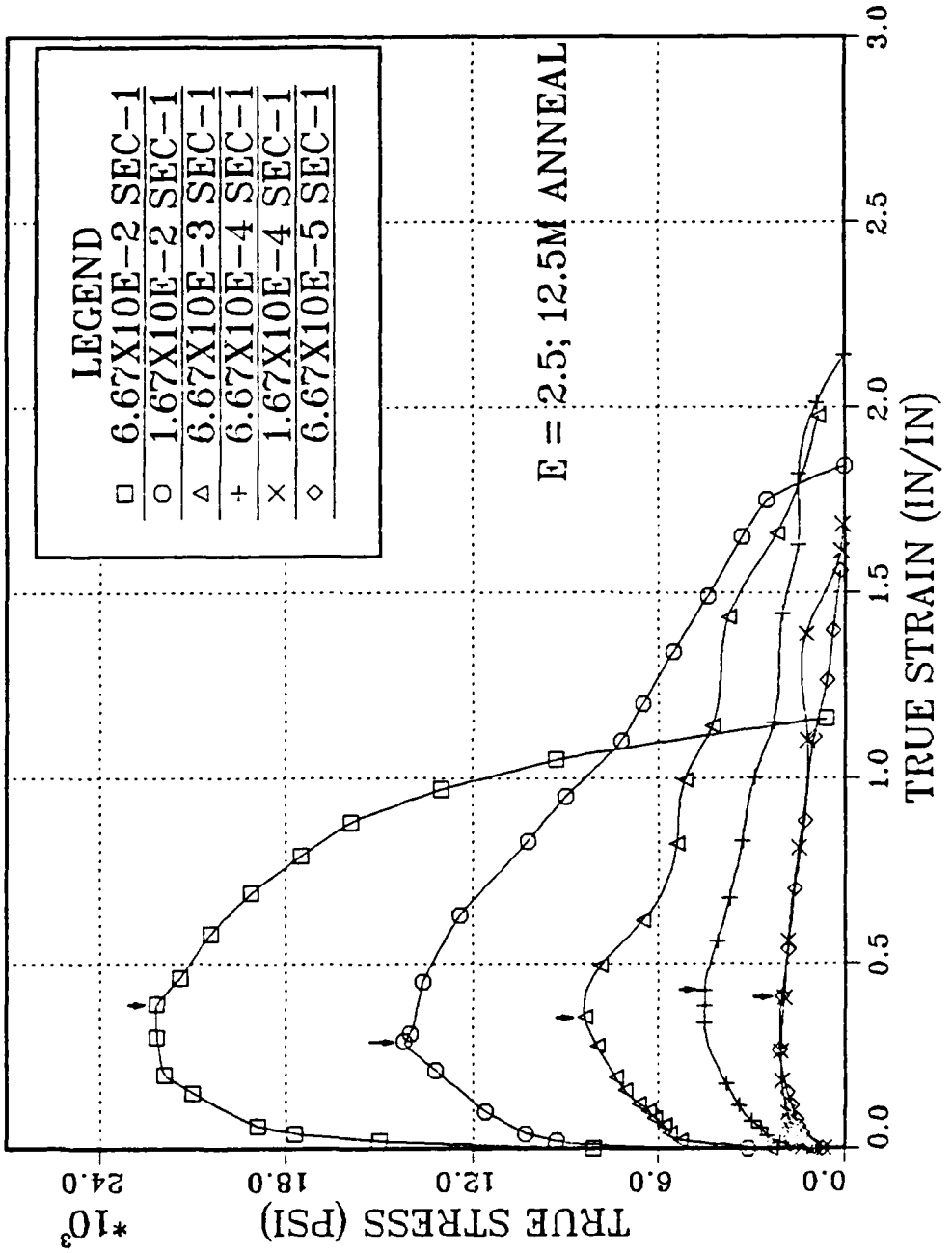

Figure 31. Stress Strain Curve for TMP D : arrow indicates point after which the relation between true stress - true strain is not strictly valid due to the onset of necking.

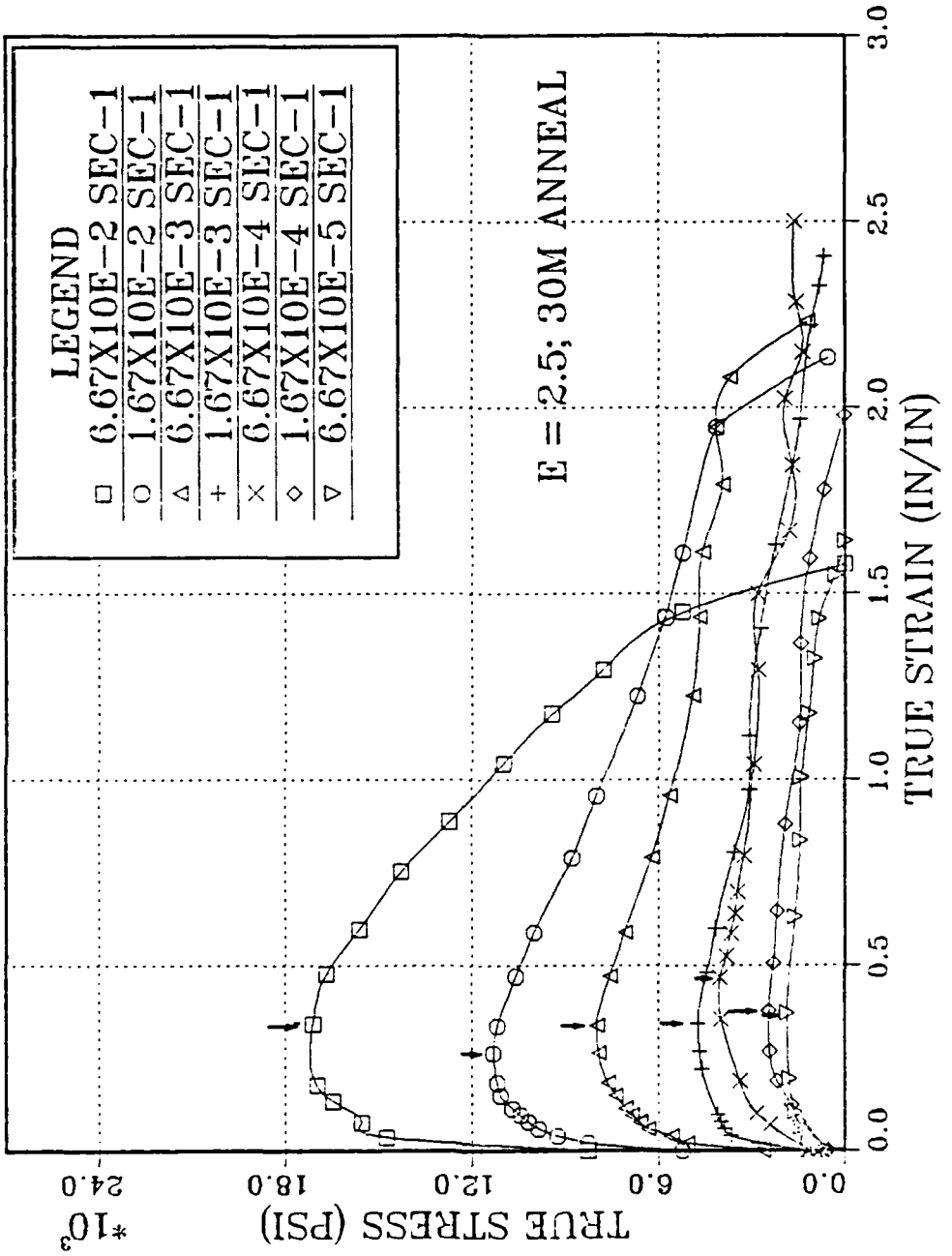

Figure 32. Stress Strain Curve for TMP E : arrow indicates point after which the relation between true stress - true strain is not strictly valid due to the onset of necking.

APPENDIX B. ENGINEERING STRESS STRAIN CURVES

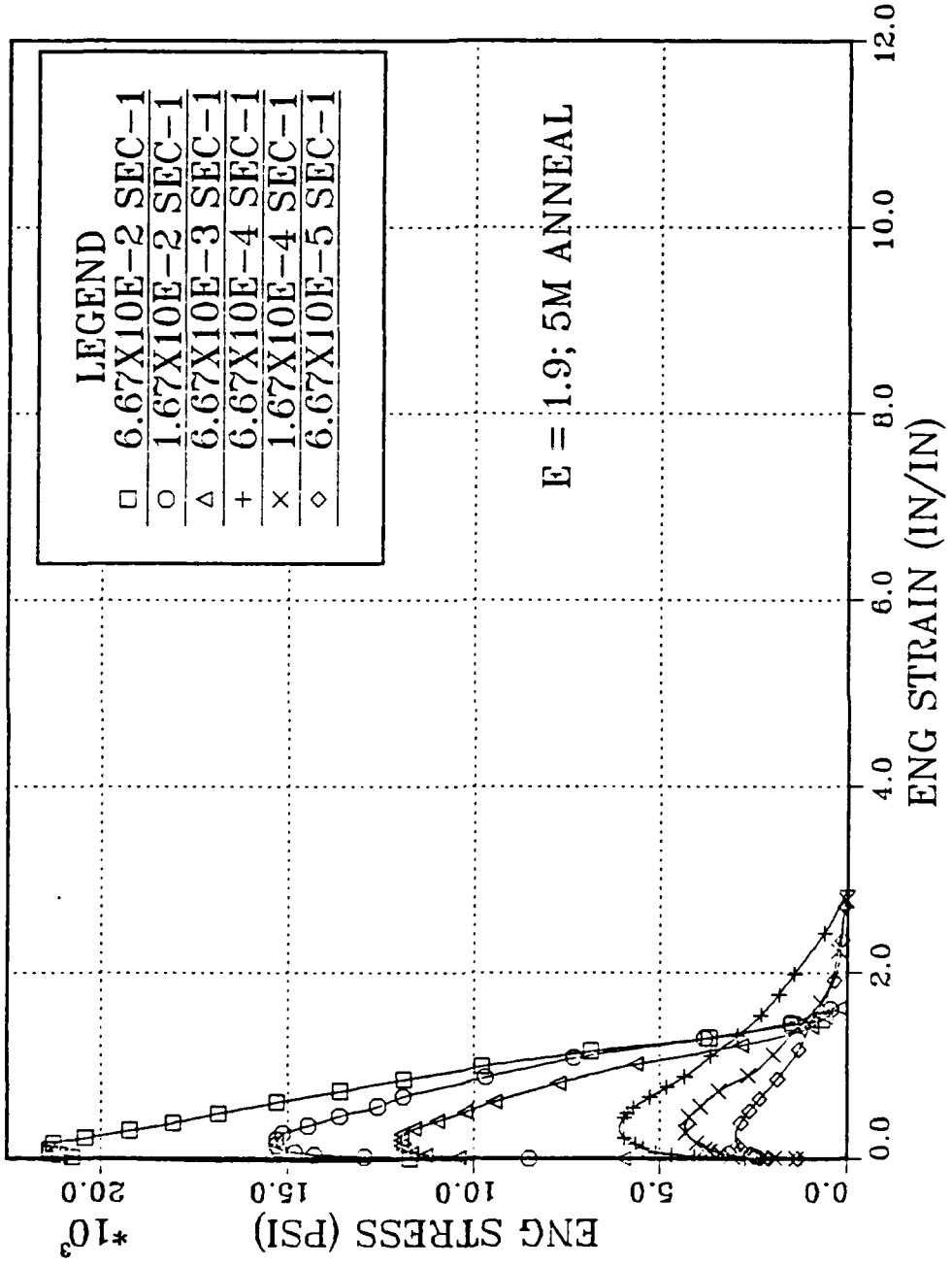

Figure 33. Engineering Stress Strain Curve for TMP A

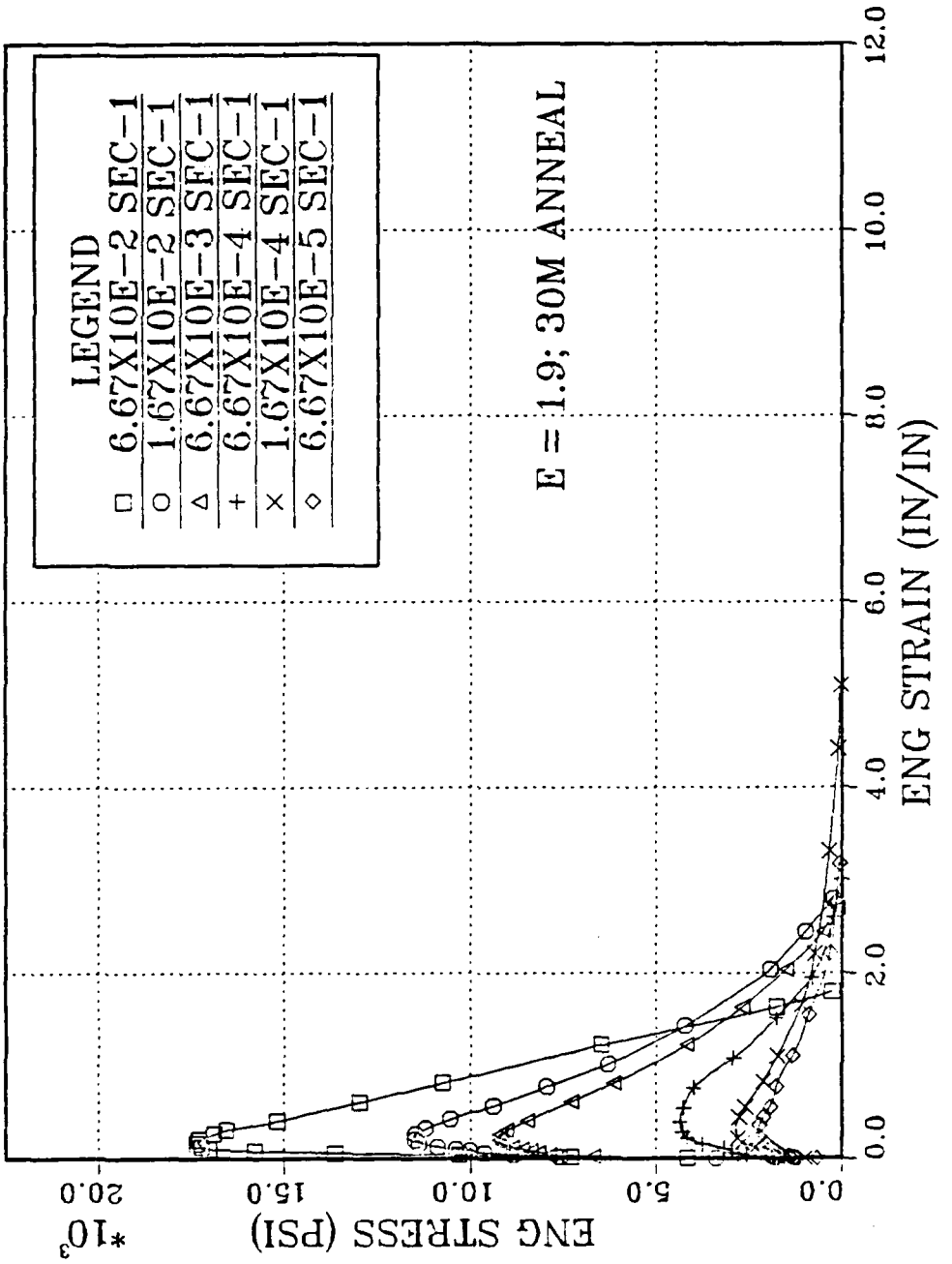

Figure 34. Engineering Stress Strain Curve for TMP B

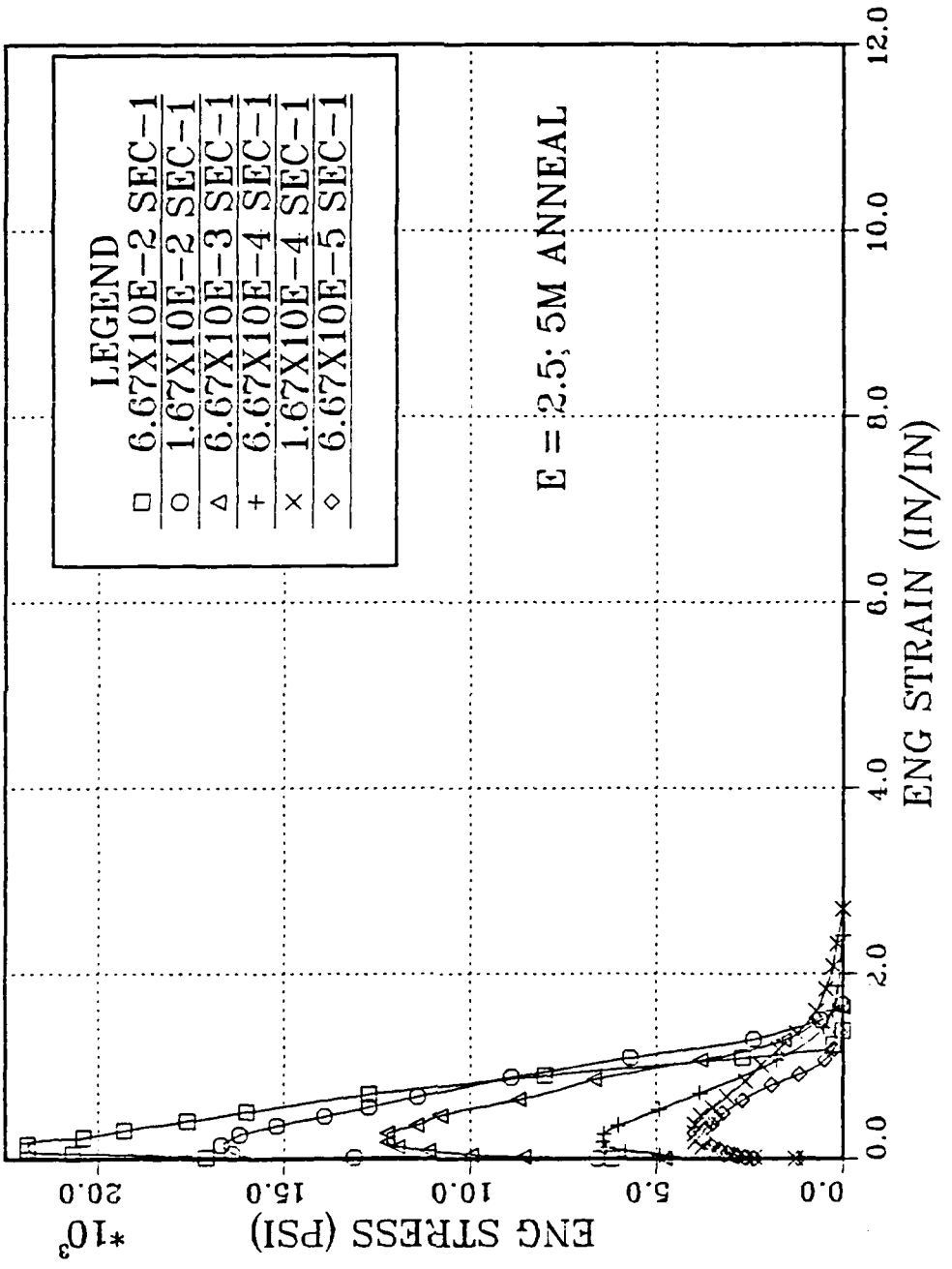

Figure 35. Engineering Stress Strain Curve for TMP C

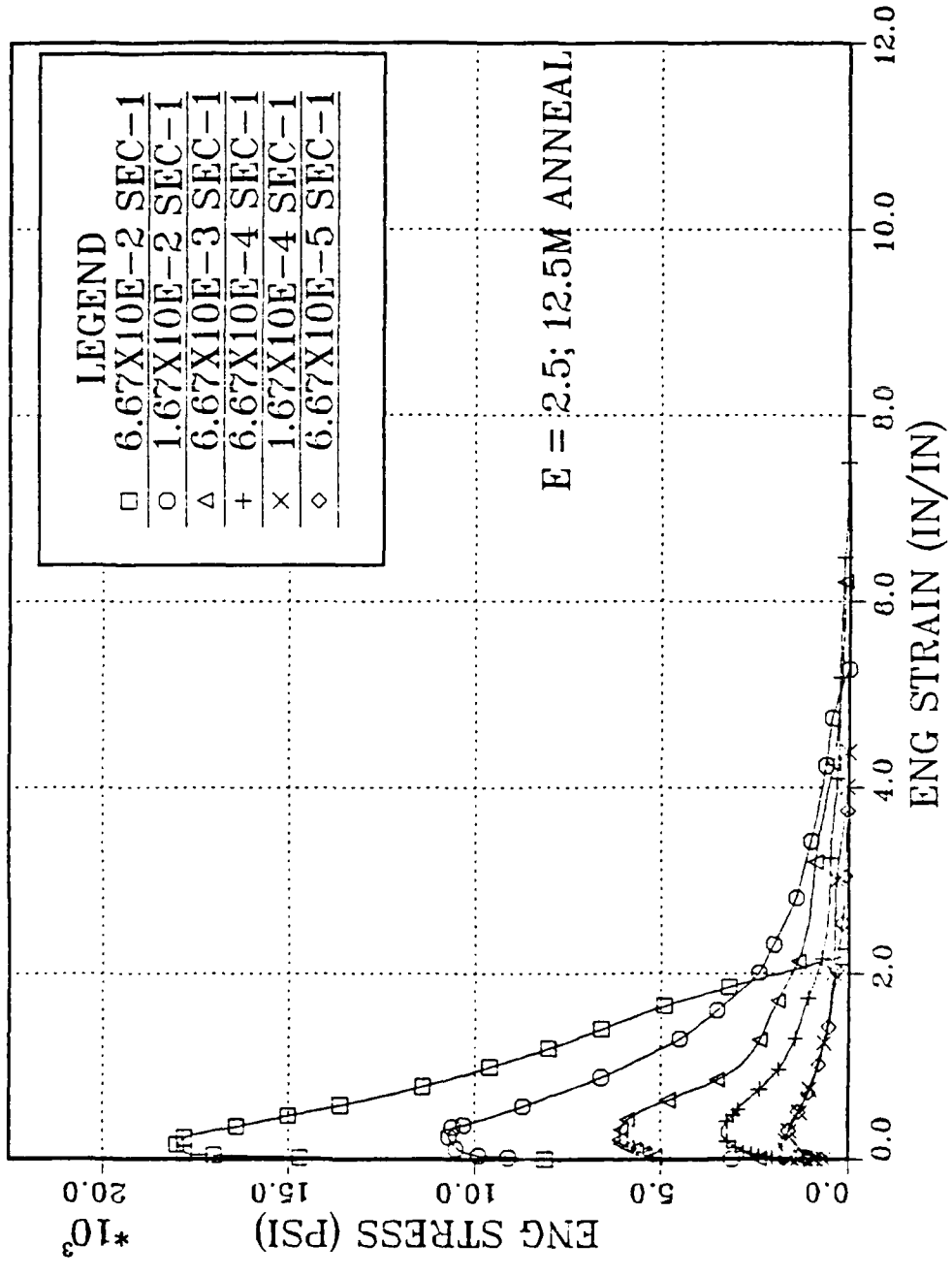

Figure 36. Engineering Stress Strain Curve for TMP D

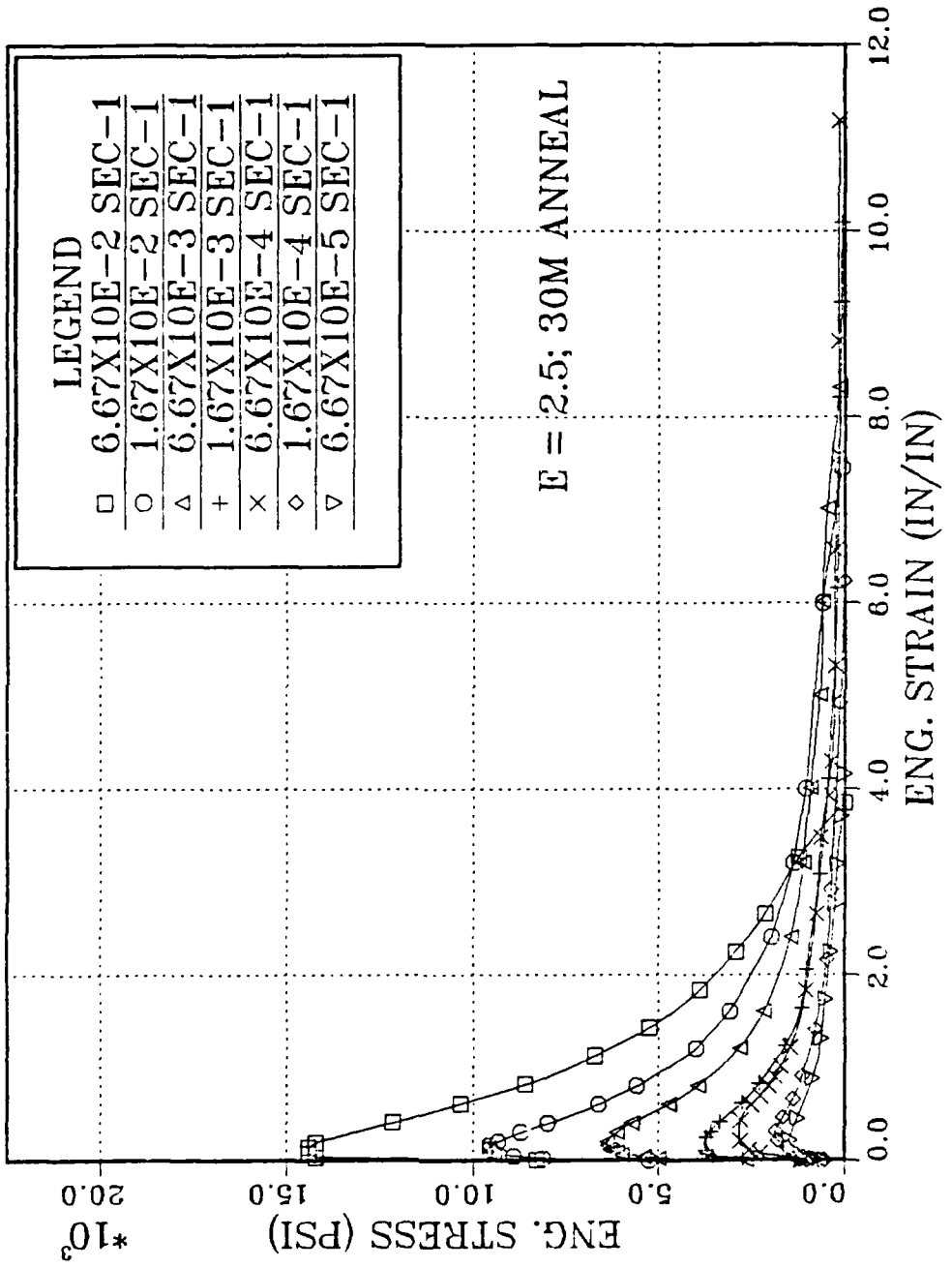

Figure 37. Engineering Stress Strain Curve for TMP E

APPENDIX C. STRAIN RATE SENSITIVITY FOR TMP'S A&B

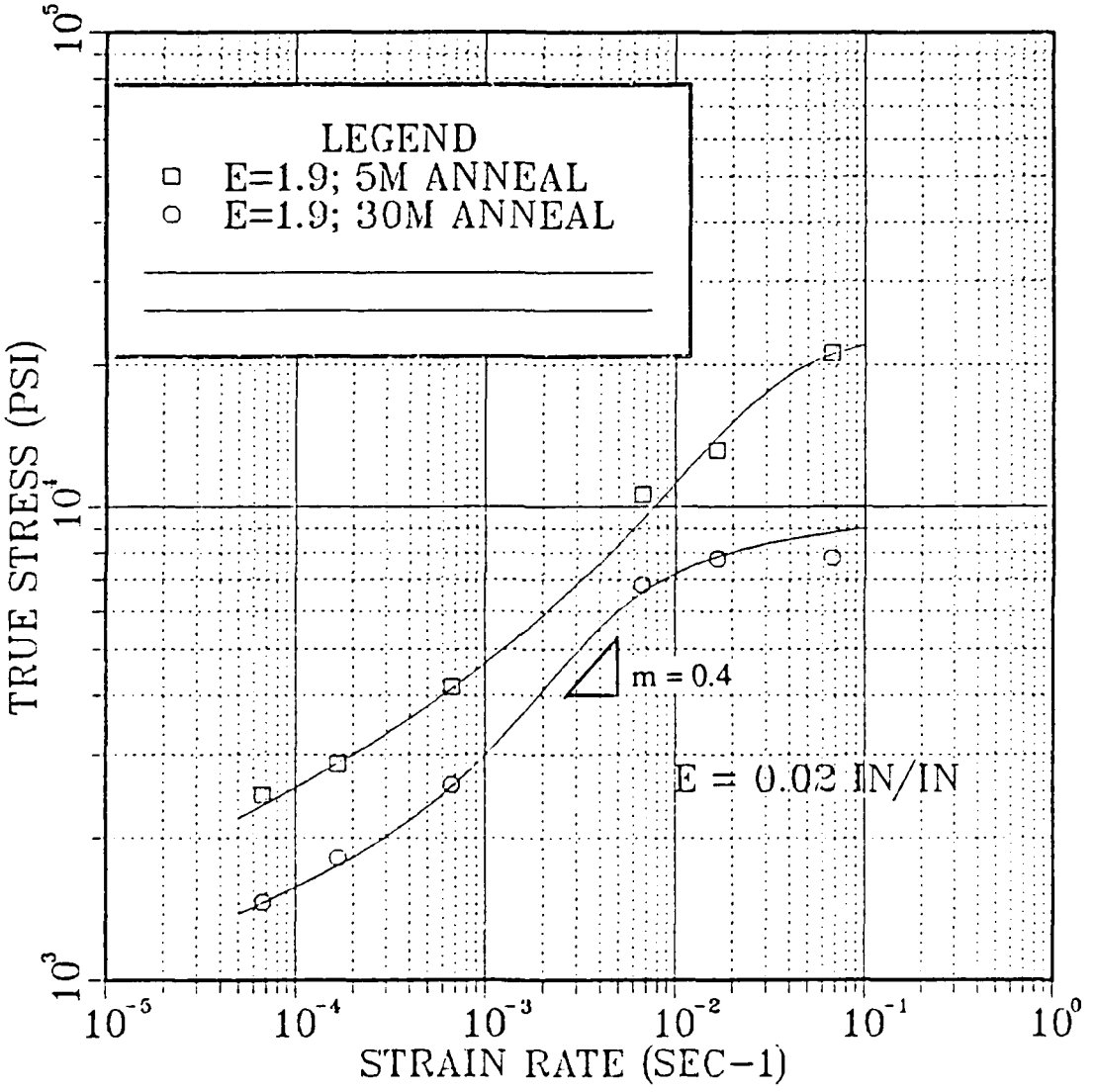

Figure 38. Strain Rate Sensitivity at ε = 0.02 for TMP A & B

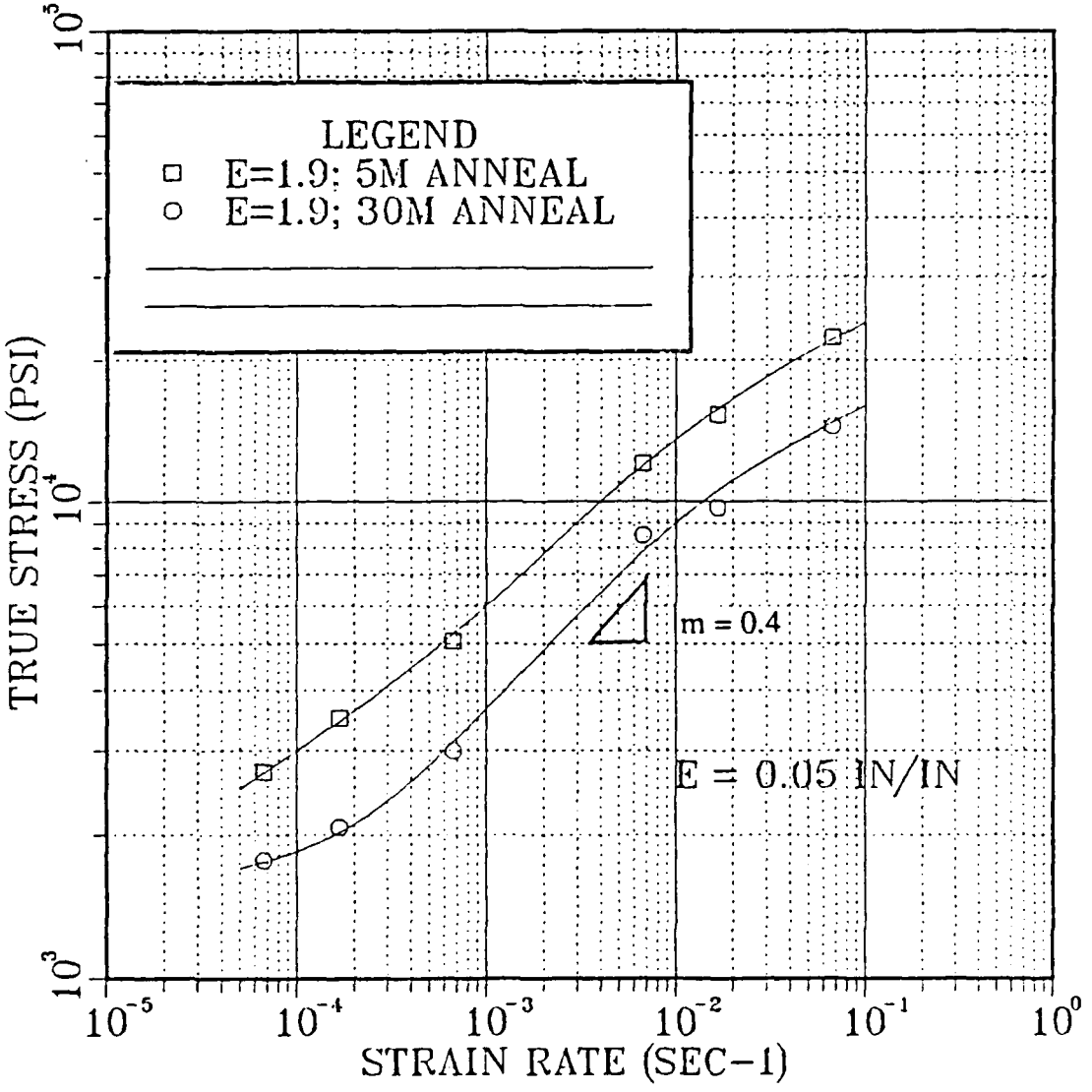

Figure 39. Strain Rate Sensitivity at ε = 0.05 for TMP A & B

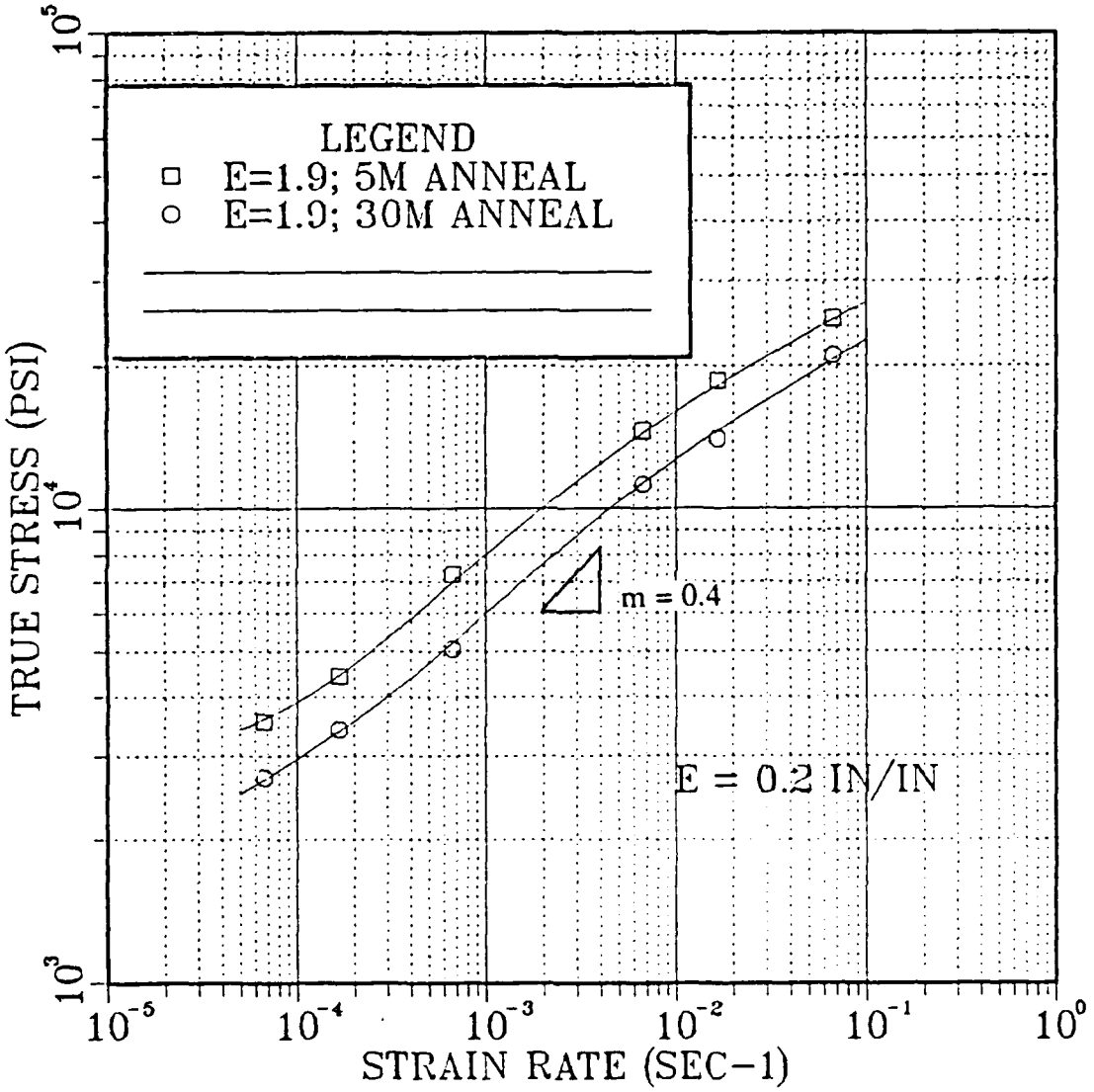

Figure 40. Strain Rate Sensitivity at ε = 0.2 for TMP A & B

APPENDIX D. STRAIN RATE SENSITIVITY FOR TMP'S C-E

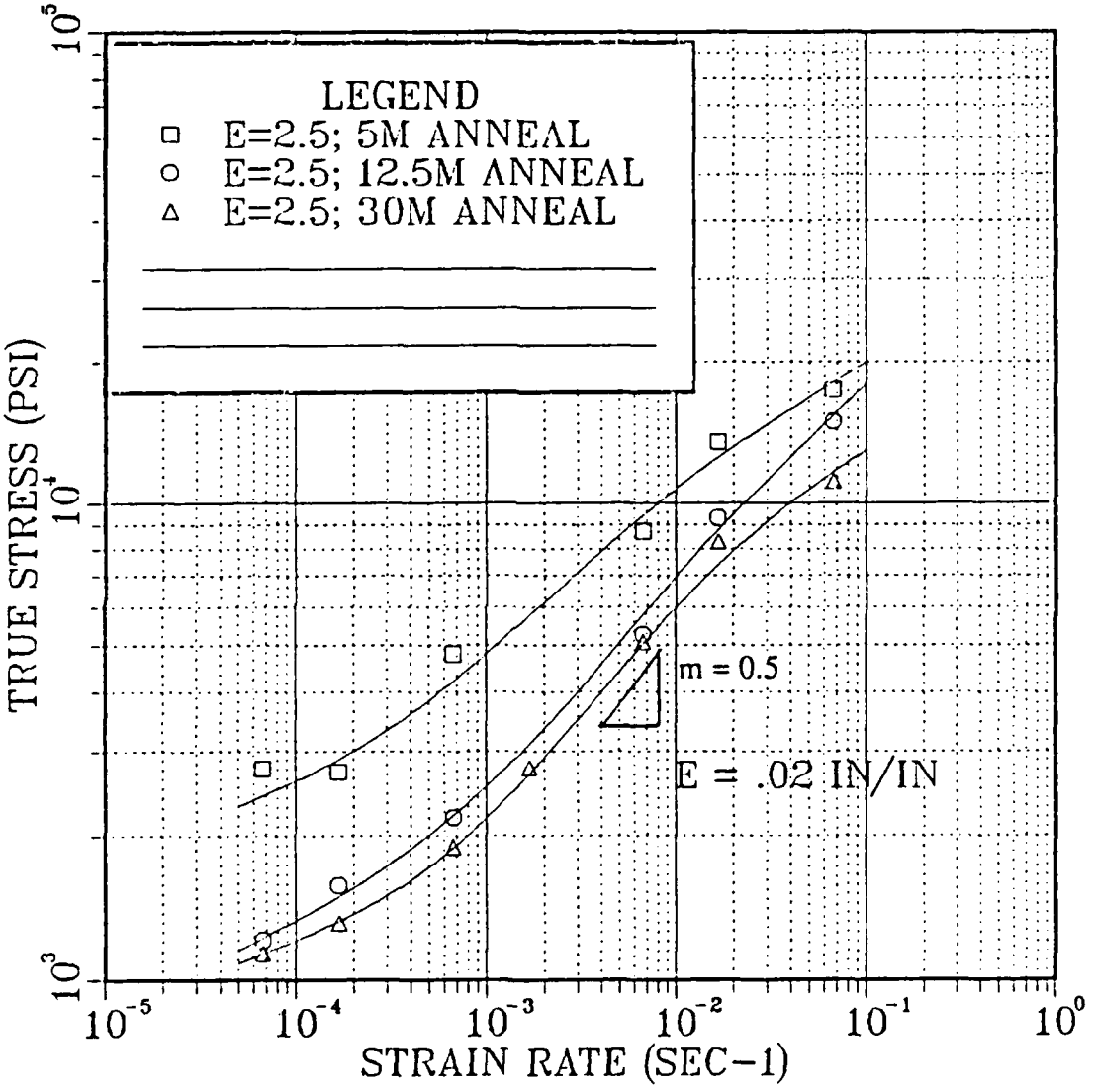

Figure 41. Strain Rate Sensitivity at ε = 0.02 for TMP's C-E

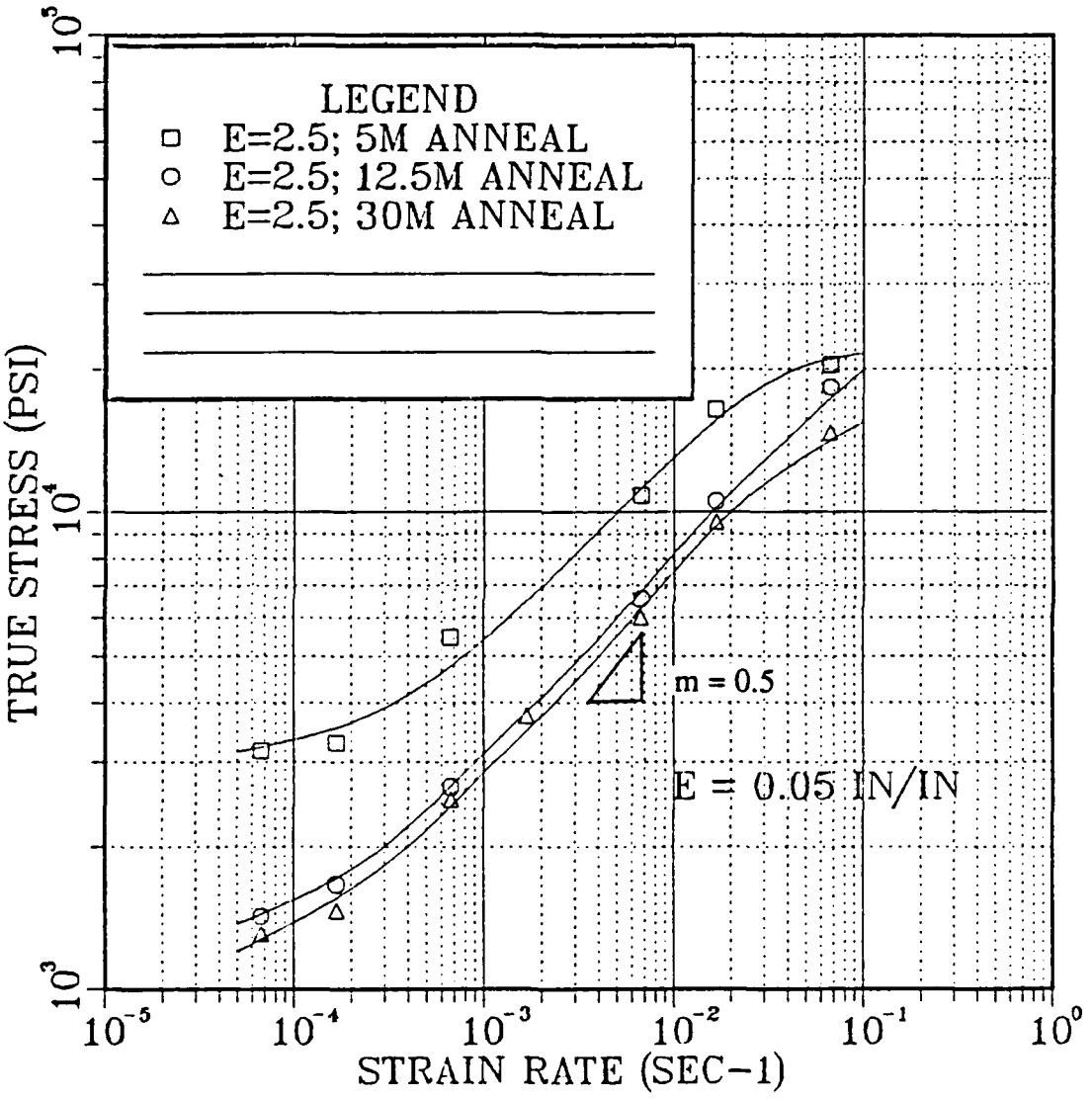

Figure 42. Strain Rate Sensitivity at ε = 0.05 for TMP's C-E

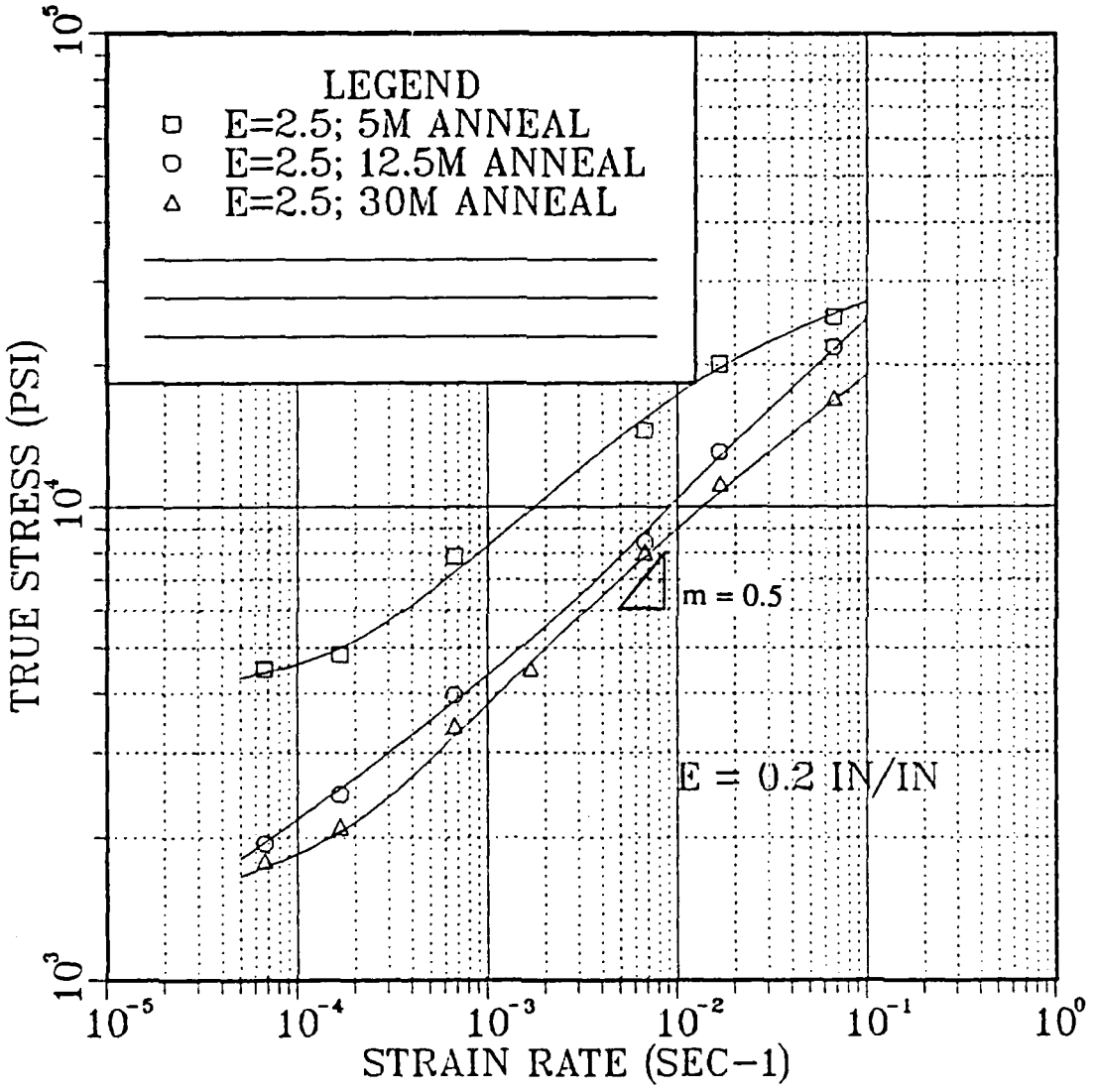

Figure 43. Strain Rate Sensitivity at ε = 0.2 for TMP's C-E

LIST OF REFERENCES

1. Bengough, G. D., "A Study of the Properties of Alloys at High Temperatures," *Institute of Metals Journal*, v. 7, 1912.

2. Underwood, E. E., "A Review of Superplasticity and Related Phenomena," *Journal of Metals*, December, 1962.

3. Watts, B. M., Stowell, M. J., Baikie, B. L., Owen, D. G. E., "Superplasticity in Al-Cu-Zr Alloys. Part I : Material Preparation and Properties," *Metal Science*, v. 10, no. 6, June, 1976.

4. *Metals Handbook*, Desk Edition, American Society for Metals, 1985.

5. Mondolfo, L. F., *Aluminum Alloys : Structure and Properties*, Butterworths, London, 1976.

6. Wadsworth, J., Pelton, A. R., and Lewis, R. E., "Superplastic Al-Cu-Li-Mg-Zr Alloys," *Metallurgical Transactions A*, v. 16A, December, 1985.

7. Sherby, O. D. and Wadsworth, J., "Development and Characterization of Fine-Grain Superplastic Materials," *Deformation, Processing and Structure*, American Society for Metals, 1982.

8. Hales, S. J. and McNelley, T. E., "Recrystallization and Superplasticity at 300°C in Al-Mg Alloys : I - Experimental Evidence," *Metall Trans.* (in review).

9. Hales, S. J. and others, "Grain Refinement and Superplasticity in a Lithium Containing Al-Mg alloy by Thermomechanical Processing," *Journal de Physique*, Colloque C3, Supplement au n°9, Tome 48, September, 1987.

10. Hales, S. J., McNelley, T. E. and McQueen, H. J., "Recrystallization and Superplasticity at 300°C in Al-Mg Alloys : II - A Qualitative Model," *Metall Trans.* (in review).

11. Hales, S. J. and McNelley, T. E., "Microstructural Evolution by Continuous Recrystallization in a Superplastic Al-Mg Alloy," *Acta Metall.*, v. 36, 1988.

12. Dieter, G. E., *Mechanical Metalurgy* , 3rd Edition, McGraw-Hill, New York, 1986.

13. Wadsworth, J., and Sherby, O. D., "Fine Grained Superplastic Materials," *Society for Advancement of Material and Process Engineering Technology*, 29th National SAMPE Symposium, April 3-5, 1984.

14. Lee, E. W. and McNelley, T. R., "Microstructure Evolution During Processing and Superplastic Flow in a High Magnesium Al-Mg Alloy," *Materials Science and Engineering*, v. 93, 1987.

15. Chester, A. P. III, *Optimizing Superplastic Response in NAVELITE, a Lithium Containing Aluminum - Magnesium Alloy*, Master's Thesis, Naval Postgraduate School, Monterey, California, 1989.

16. Monroe, I. B., *Optimizing Superplastic Response in Lithium Containing Aluminum - Magnesium Alloys,* Master's Thesis, Naval Postgraduate School, Monterey, California, 1987.

17. Abou - Salama, A. A., *Analysis of Grain Refinement and Superplasticity in Aluminum - Magnesium Alloys*, Ph.D. Dissertation, Naval Postgraduate School, Monterey, California, 1987.

18. Hales, S. J. and McNelley, T. E., "Fined Grained Superplasticity at 300°C in a Wrought Al-Mg Alloy," *Superplasticity in Aerospace,* TMS - AIME, Warrendale, Pennsylvania, 1988.

19. Hales, S. J., McNelley, T. E., and Crooks, R., "Continuous Recrystallization During Thermomechanical Processing of a Superplastic Al-10Mg-0.1Zr Alloy," *Proceedings of the International Conference on Recrystallization in Metallic Materials,* in press, TMS - AIME, Warrendale, Pennsylvania, 1990.

20. Weinberg, F. A., "Grain Boundary Shear in Aluminum," *Transactions of the Metallurgical Society of AIME,* V. 212, 1958.

INITIAL DISTRIBUTION LIST

	No. Copies
1. Defense Technical Information Center Cameron Station Alexandria, Virginia 22304-6145	2
2. Library, Code 0142 Naval Postgraduate School Monterey, California 93943-5002	2
3. Weapon Systems Engineering Curricular Office, Code 33 Naval Postgraduate School Monterey, California 93943	1
4. Professor T.R. McNelley, Code 69Mc Department of Mechanical Engineering Naval Postgraduate School Monterey, California 93943	5
5. Dr. Eui-Whee Lee, Code 6063 Naval Air Development Center Warmister, Pennsylvania 18974	1
6. Dr. Lewis E. Sloter, Code AIR 931A Headquarters, Naval Air Systems Command Washington, D.C. 20361	2
7. LCDR Thomas E. Gorsuch 49 Greenview Ave. Reisterstown, Maryland 21136	2